Aquifer Characterization in the Blue Ridge Physiographic Province

William J. Seaton

Dissertation submitted to the Faculty of the

Virginia Polytechnic Institute and State University

in partial fulfillment of the requirements for the degree of

DOCTOR OF PHILOSOPHY

in

GEOLOGICAL SCIENCES

Thomas J. Burbey, Chair

Cahit Çoruh

William S. Henika

John A. Hole

Jeffrey A. Johnson

A. Krishna Sinha

January 25, 2002

Blacksburg, Virginia

Keywords: Blue Ridge Province, aquifer, hydrogeology, electrical resistivity, borehole geophysics

Aquifer Characterization in the Blue Ridge Physiographic Province

by

William J. Seaton

(ABSTRACT)

Existing models of the hydrogeology in the Blue Ridge Province in the eastern United States generally assume a simplified two-layered system consisting of shallow unconsolidated and relatively homogeneous and porous regolith with a water-table aquifer that slowly supplies water downward to the underlying variably fractured crystalline bedrock. In these models, interconnected fractures in the crystalline bedrock act as conduits for predominantly downward vertical and limited horizontal flow. Fracture density is depth–limited and correlated with proximity to topographic lineaments. Current models consider the porous regolith as the primary water storage reservoir for the entire aquifer system.

In this research, detailed hydrogeologic studies in the Blue Ridge Province in Floyd County, Virginia reveal a substantially different framework for groundwater flow. Recent acquisition of two-dimensional surface resistivity profiles collected using a variety of array techniques combined with borehole geophysical logs revealed new insights into this geologically complex province. Dipole-dipole arrays were particularly important in gathering high resolution resistivity profiles that document horizontal and vertical resistivity variation reflecting changes in subsurface geology and anomalous low resistivity areas in crystalline bedrock associated with fault zones.

The shallow regolith contains unsaturated areas and also localized sand and clay prone facies with water table and confined aquifer conditions residing locally. Hydraulic heads between the shallow aquifer and the deeper fractured bedrock aquifer can vary by 20 m vertically. Within the crystalline bedrock are anomalous lower resistivity intervals associated with ancient fault shear zones. Brecciated rock adjacent to the shear zones, and the shear zones themselves, can be hydraulically conductive and serve as pathways for groundwater movement. Aquifer testing of the regolith-bedrock fracture system occurred over a 6-day period and produced rapid and relatively uniform drawdowns in surrounding wells completed in the fractured bedrock aquifers. The shallow aquifers experienced minimal drawdowns from the aquifer test indicating low vertical hydraulic conductivity and limited communication between the shallow and deeper bedrock aquifers. Water chemistry and chlorofluorocarbon (CFC) age dating analyses indicated significant differences between water samples from the shallow and deep aquifers. A new conceptual model for Blue Ridge aquifers is proposed based on these research findings.

GRANTS

This work was funded by research grants from the Virginia Water Resources Research Center (VWRRC) and the Department of Geological Sciences at Virginia Tech, which are gratefully acknowledged.

DEDICATION

This work is dedicated to my parents Bob and Pat Seaton. Thanks Mom and Dad for your tireless efforts in raising your six kids and for showing us the value of an education.

ACKNOWLEDGEMENTS

I would like to thank my advisor, Tom Burbey, for his friendship and assistance throughout our time together at Virginia Tech. Tom was instrumental in acquiring the essential geophysical equipment and the major funding for this research as well as editorial, technical, and general moral support. I also thank Cahit Çoruh, Bill Henika, John Hole, Jeff Johnson, and Krishna Sinha for their generous assistance and suggestions as members of my committee. Thanks also to Lynn Glover III and John Costain for providing vision and guidance early in the life of this project. John Costain was particularly instrumental in capturing my interest in using geophysics with hydrogeology.

Many thanks to Lynwood and Evelyn Drake for allowing us to use their beautiful farm in the Blue Ridge Mountains as a field site for this research. Thanks also to Todd and Vicki Via for their help at the Drake farm. Thanks to Kenneth Pauley of Pauley Drilling Co., Doug Woods of Copper Hill Daycare, and Ben Williams for allowing access to their properties. Many insights for this work came from discussions with Paul Haynes of Haynes Drilling Co. in Christiansburg, Virginia. Thanks to Ted Dean of ATS International, Inc. for his help and lending of equipment. Thanks to Ben Dozier and Miles Gentry for their help at the field site. Thanks to Dave Nelms and his team from the USGS Water Resources Division who collected water samples for analysis and age dating and to Neil Plummer for the sample analysis. John and Mark Wonderly and Mark Lemon provided valuable assistance with maintenance of the field equipment.

Connie Lowe, Mary Mc Murray, Linda Bland, and Carolyn Williams provided essential help with the logistics of being a graduate student at Virginia Tech.

I am very thankful to my wife Terry and my children Kelly, Kevin, Patrick, and Ann for their love, faithfulness, and patience.

The greatest thanks and praise goes to my Lord and Savior Jesus Christ. He came to Earth to show us exactly what God is like, and then He died for our sins so that we all could have the opportunity to share eternity with Him. He is the Living Water who bids each one of us to come and drink. Thank you Jesus!

CONTENTS

TABLE OF FIGURES

INTRODUCTION

This dissertation is composed of three independent chapters that are associated with the characterization of aquifers in the Blue Ridge Physiographic Province. Each chapter was written for publication in a peer-reviewed professional journal. At the time of this dissertation, Chapter 1 has been published (Seaton and Burbey, 2000), Chapter 3 is in review by the Journal of Applied Geophysics, and Chapter 2 is being prepared for publication.

Chapter 1 presents an analysis of the hydrogeology of the Blue Ridge Province at the field site based on geological and geophysical evidence. The use of two-dimensional resistivity profiles, borehole geophysics, and lineament analysis allows the correlation of thrust faults in the subsurface with fractured bedrock aquifers. In addition, the resistivity profiles reveal details about the complex nature of the shallow regolith and its role in the flow of groundwater.

Chapter 2 discusses the results of a six-day aquifer test at the field site, chemical analysis of water samples from the shallow and deep aquifers, and age dating of the groundwater. This information provides the basis for a new conceptual model of aquifers in the Blue Ridge Province. The new model incorporates findings in the Blue Ridge Province from North Carolina, Georgia, and Maryland as well as observations from water well drillers and other water resource personnel.

Chapter 3 is an investigation of the methods used to collect data for the resistivity profiles used in this study. Comparison of Wenner, Schlumberger, dipole-dipole, and pole-pole arrays reveals that the dipole-dipole data produces inversion results with the most subsurface detail, highest resolution, and the greatest depth of penetration. Dipole-dipole arrays were used exclusively throughout this research as a result of this investigation.

The new conceptual model proposed herein will provide hydrogeologists, municipalities, regulators, and other water resource personnel with an up-to-date “template” for making informed decisions concerning the location, quantity, and use of groundwater in the Blue Ridge Province.

Chapter 1: Geologic Analysis of Aquifers in the Blue Ridge Physiographic Province Using Resistivity Profiling and Borehole Geophysics

ABSTRACT

Existing hydrogeological models used to describe the recharge and movement of groundwater in the Blue Ridge Province in the eastern United States generally rely on a simplified two-layer system consisting of regolith overlying a fractured bedrock aquifer. The regolith in these models is assumed to be relatively homogeneous and contains a water table aquifer that supplies water to the underlying variably fractured homogeneous crystalline bedrock. The interconnected fractures in the bedrock serve as conduits for predominantly downward vertical and limited horizontal flow.

Recent acquisition of two-dimensional surface resistivity profiles and borehole geophysical logs has revealed new insights into this geologically complex province. The shallow regolith contains large unsaturated areas and also localized sand and clay prone facies with water table and confined aquifer conditions residing locally. Within the crystalline bedrock are anomalous lower resistivity intervals that are associated with ancient fault shear zones. These shear zones intercept the regolith-bedrock interface at high angles and become more horizontal with depth. Brecciated rock adjacent to the shear zones, as well as the shear zones themselves, can be hydraulically conductive and serve as pathways for vertical and horizontal groundwater movement from source-recharge areas to distant wellbores.

Regolith and aquifer-property characterization from geophysical and hydrological data acquired in this investigation has allowed reasonable conclusions to be drawn about groundwater movement in the Blue Ridge Province for water supply, contaminant transport, and watershed/wellhead protection delineation.

INTRODUCTION

The Blue Ridge Physiographic Province is an elongate belt of structurally and stratigraphically complex metamorphosed igneous and sedimentary rocks extending from Pennsylvania through western Virginia to Georgia. The area where this research was conducted (herein termed “field site”) is located 30 kilometers southwest of Roanoke, Virginia, near the western edge of the Blue Ridge Province in Floyd County, Virginia. The Blue Ridge Province is located west of the Piedmont Province and east of the Valley and Ridge Province (fig. 1.1). The Piedmont and Blue Ridge provinces are usually considered a single groundwater region because of their hydrologic and geologic similarities (e.g., LeGrand, 1967, Heath, 1984). This paper presents a study of the geologic framework of the aquifers in the Blue Ridge Province in the area of interest.

Finding adequate water resources for homeowners and municipalities in this region has historically been a difficult task. Water wells often have unacceptably low yields. High yielding wells necessary for rural municipalities or larger developments have proven to be difficult to locate and represent a small minority of the total number of wells in use. Although no comprehensive database exists for Blue Ridge water wells yields, an estimated 10-15 % of the wells drilled could be classified as “dry holes”. Maximum yields rarely exceed 25 gallons-per-minute (GPM) (personal communications with water well drillers and health department personnel, Floyd and neighboring counties, 1999).

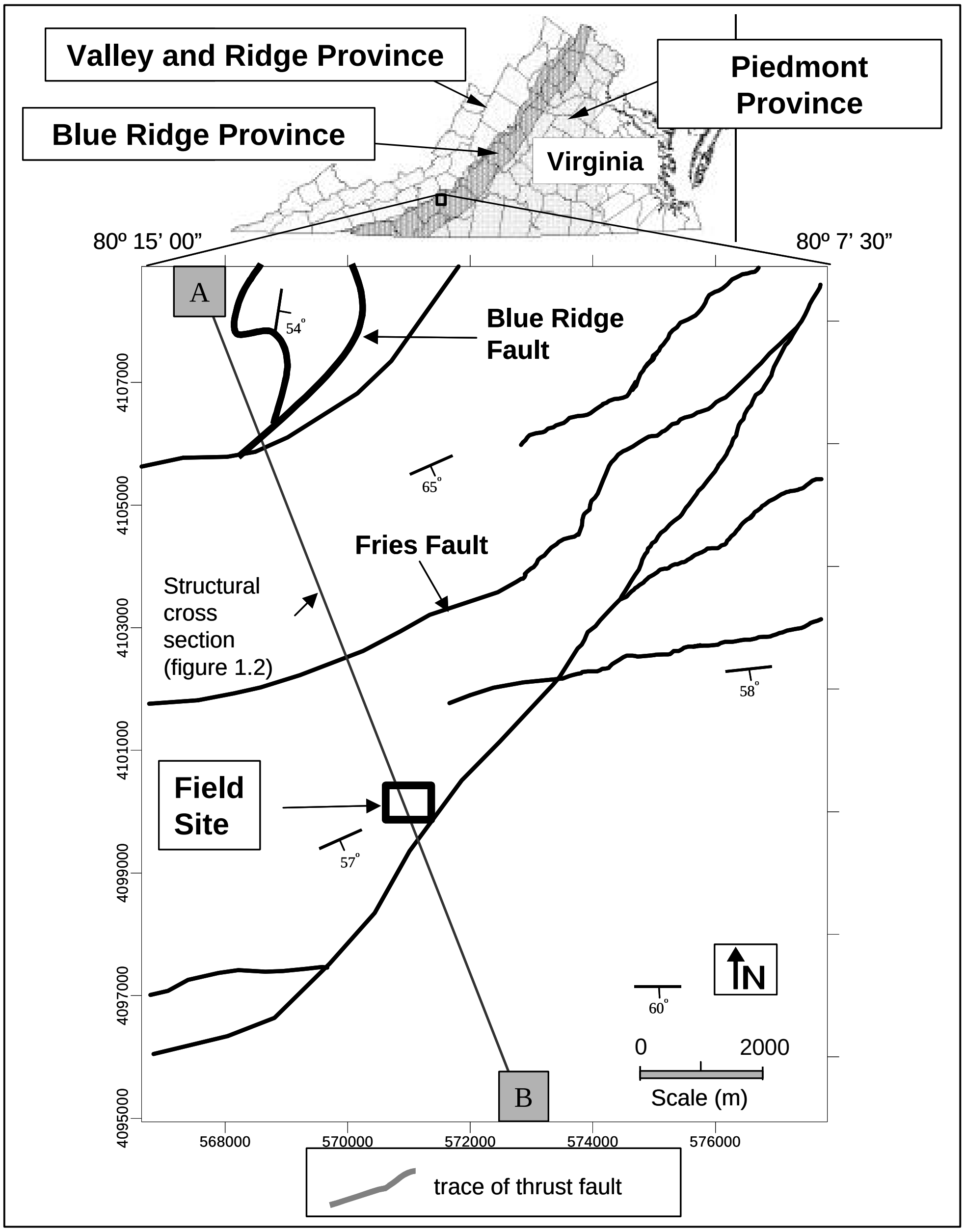

Figure 1.1 Location of the field site in the Check Quadrangle, Blue Ridge Physiographic Province, Floyd County, southwest Virginia. Traces of thrust faults and strike-dip data from Walsh-Stovall, et al., (2000). Structural cross section A-B illustrated in figure 1.2.

The generally poor success rate of drilling wells that yield acceptable quantities of water is partially due to the methods used to select drilling locations. Water well drilling sites are often selected to satisfy regulations regarding minimum distances from septic systems or other sources of surface contamination without consideration of the underlying geology. Water "witching" is still commonly employed in rural areas. Detailed groundwater resource studies are often limited to the analysis of geomorphology and surface structural lineaments because of the lack of suitable outcrops and the complex subsurface environment in this region (Daniel, 1989). When contamination problems in water resources arise, it is often difficult to determine contaminant source areas because of the limited understanding of recharge and subsurface flow systems in this area.

The conceptual models used to characterize the Blue Ridge Province are often simplistic. These models assume a relatively homogeneous unconsolidated layer of soil and weathered rock containing a water table aquifer supplying water to underlying variably fractured homogeneous crystalline bedrock. Interconnected fractures are thought to serve as conduits for predominantly downward vertical and limited horizontal flow. The primary sources of geologic data used to conceptualize the Blue Ridge Province have been field observations from limited bedrock outcrops and shallow (< 100 m) water wells and interpretation of surface lineaments from high-altitude photographs. Published aquifer tests in terranes similar to the Blue Ridge indicate a variety of scenarios. Gernand and Heidtmann (1997) found heterogeneous aquifers composed of many interconnected low-permeability fractures in a relatively impermeable matrix. Maximum drawdowns from long-term pump tests did not parallel the most abundant fracture set, demonstrating limited correlation between major structural features and the hydraulic response during pumping. Daniel and Sharpless (1983) determined the cone of depression in the water table aquifer above fractured bedrock in the Piedmont of North Carolina to be aligned with the principal joint set in the bedrock. Donn, et al, (1989) associated elongated drawdown contours created by pumping a Piedmont aquifer to be aligned with a fracture trend or igneous intrusion in the bedrock.

In this study, two dimensional surface resistivity profiles and geophysical borehole logs were acquired to investigate the geologic constraints on groundwater recharge and flow. This geophysical information is incorporated with water well data, geologic data from outcrops and boreholes, interpreted structural lineaments from computer generated shaded-relief topographic maps, and hydraulic test measurements. The integration of these sources of information has provided a more detailed picture of the subsurface allowing a reassessment of the conceptual groundwater models used to describe the aquifers in this province (Griffiths and Barker, 1993; Paillet, 1995). In particular, the 2-D surface resistivity profiles provide a new approach to study the regolith and bedrock zones. When utilized with other types of data, resistivity profiles provide new insights into the subsurface in a manner not previously possible.

GEOLOGICAL HISTORY

The Blue Ridge Province is composed of Late Proterozoic through Paleozoic metasedimantary and metavolcanic rocks that were deposited on middle Proterozoic basement. The metasedimantary and metavolcanic rocks were metamorphosed to greenschist facies during the middle to late Paleozoic. The basement rocks were metamorphosed to granulite facies during the Precambrian Grenville Event. The current geologic setting in the Blue Ridge is a composite of repeated compressional and extensional tectonism from Pre-Cambrian through late Paleozoic time. Bedrock consists of layered granulite gneiss, granitic gneiss, augen gneiss, massive, highly fractured vein quartz, and phyllonitic mica-schist that generally strikes to the northeast and dips steeply to the southeast. Phyllite and quartzite of the Chilhowie Group outcrop along the western margin of the Blue Ridge Province. The Blue Ridge metamorphic rocks in Floyd County are within a system of generally northeast striking thrust faults stacked vertically and shingled laterally. The oldest thrust sheets have undergone multiple periods of extensional and compressional deformation throughout the Paleozoic era and have been crosscut by younger extensional strike-slip faults and diabase dikes. The Blue Ridge Fault underlies Floyd County and is the primary decollmont separating the over-thrusted Precambrian metamorphic rocks of the Blue Ridge Province from the underlying Paleozoic age sedimentary rocks that outcrop in the Valley and Ridge Province (Fig. 1.2, Henika, 1981, 1992, 2000; Bartholomew and Lewis, 1984; Bartholomew, et al., 1999, Walsh-Stovall et al., 2000).

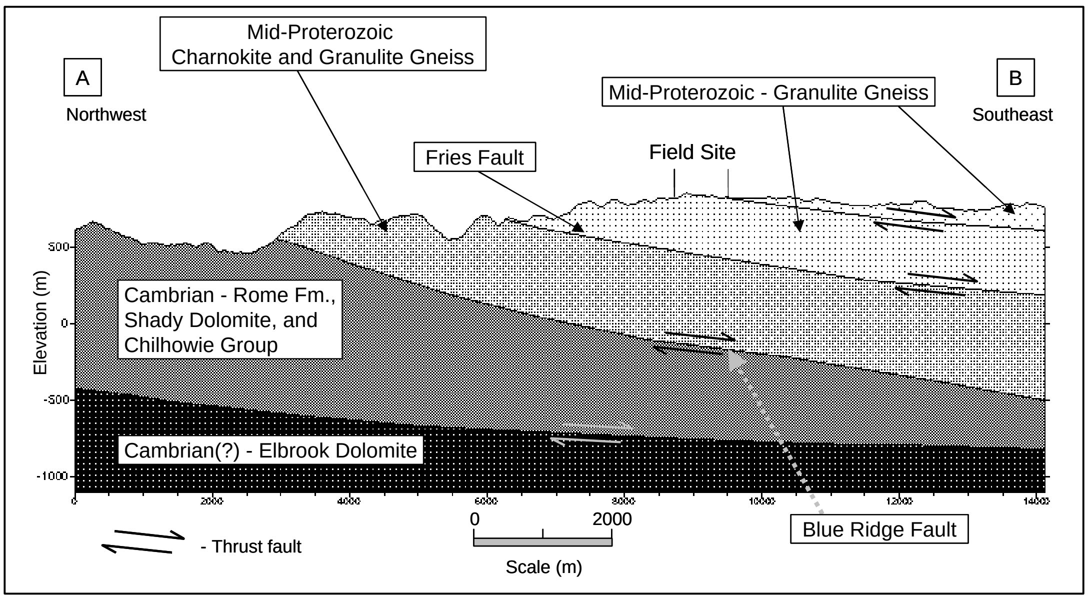

Figure 1.2 Simplified structural geologic cross section A-B through the overthrusted Blue Ridge metamorphic rocks in the Check quadrangle in southwest Virginia. (Walsh-Stovall, et al., 2000, Bartholomew, et al., 2000)

Lineament analysis of the shaded-relief digital elevation model (DEM) for the field site (Check, Virginia, 7.5 minute quadrangle) reveals numerous north-south and northwest-southeast oriented joints that formed during the later stages of Appalachian tectonism (Fig. 1.3 a,b, Walsh-Stovall et al., 2000). Northeast-southwest oriented linear features associated with early Blue Ridge thrust faulting can also be detected (Fig. 1.3c).

Bedrock is overlain by a variably thick (0-35 m) soil and saprolite zone (herein termed "regolith") originating from the weathering of the underlying bedrock. Massive quartz and

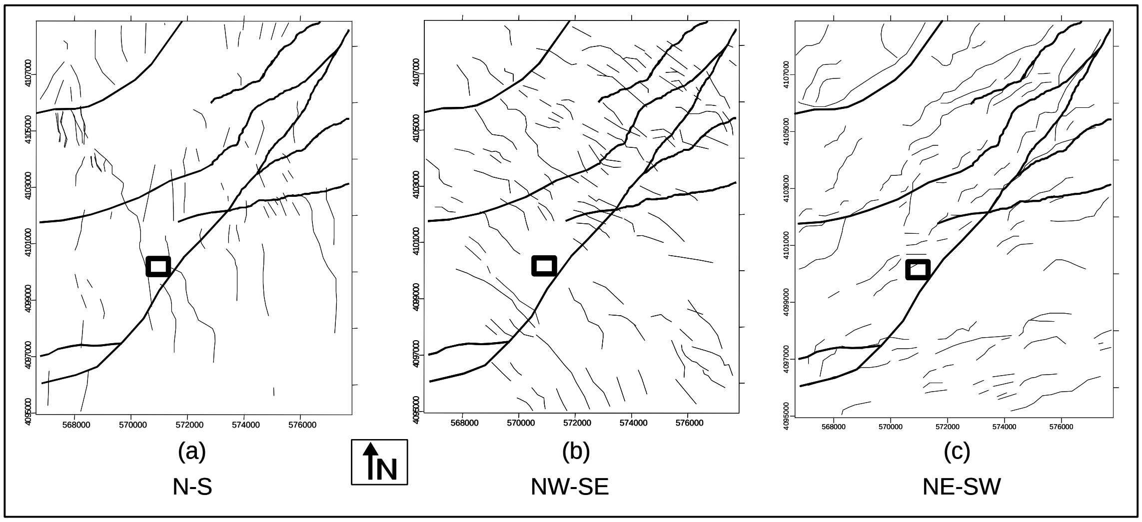

Figure 1.3 North-south (a), northwest-southeast (b), and northeast-southwest (c) oriented lineaments interpreted from the Check, Virginia, 7.5 minute USGS quadrangle. The field site in each frame is represented by the black rectangle.

quartz-rich granitic gneiss is the most resistant to weathering; biotite and augen gneiss weather more readily and produce the thickest regolith. Phyllonitic mica-schist forms resistant clays when weathered and can be found underlying many of the low relief hills in the Blue Ridge Province. Phyllonitic mica-schist and fractured gneiss (Fig. 1.4) are considered to represent the fault plane surfaces and adjacent overlying intensely disturbed fault zones that can serve as conduits for vertical and lateral flow of groundwater (W.S. Henika, Virginia Division of Mineral Resources, oral communication, 1999).

Figure 1.4 Outcrop of a faulted phyllonitic mica-schist shear zone in the vicinity of the field site. Mica-schist weathers quickly to a soil-like material allowing rapid plant growth.

METHODS

Surface resistivity profiles

Surface resistivity methods have been used for groundwater research for many years. Earth resistivities are related to important geologic parameters of the subsurface including types of rocks and fluids present, porosity, and degree of saturation (Griffiths and Barker, 1993). Studies by Brown (1996), Isiorho and Nkersuwem (1996), Janardhana et al., (1996), Choudhury, et al., (1997) have analyzed structural features such as fractures and lineaments with resistivity surveys in a variety of geologic settings. Lower resistivity anomalies detected by resistivity surveys are often correlated with the presence of high hydraulic conductivities or fracture permeability in the search for water supplies. However, the majority of these studies utilize one-dimensional resistivity soundings to estimate the earth resistivity beneath a single point on the surface. Several soundings are conducted over a site in an attempt to gain an understanding of the spatial distribution of resistivities and water prone areas. The resistivity sounding method assumes that the earth is composed of horizontal layers using a one-dimensional model to interpret the subsurface. Lateral changes in resistivity associated with complex geologic settings can lead to apparent resistivity values that can be easily misinterpreted. Haeni, et al. (1993) used inverted two-dimensional resistivity profiles with other surface geophysical techniques to detect fractured zones in crystalline rock. Dahlin (1996) explored both crystalline and sedimentary rocks with two-dimensional resistivity profiles relating lithologic changes seen in boreholes with inverted resistivity data.

In this study, two-dimensional surface resistivity profiles were collected using a Campus Geopulse earth resistivity meter connected to one or two multi-electrode cables utilizing 25 or 50 electrodes respectively. Dipole-dipole arrays were used throughout the study with 2, 6, or 10 m electrode spacing (see Appendix A). This technique measures a series of apparent resistivities, both vertically and horizontally in the subsurface that are later converted to a model of “true” two-dimensional earth resistivities using linear inversion modeling (Loke and Barker, 1996; Loke, 1999). Two-dimensional surface resistivity profiling accounts for the spatial variation in earth resistivities associated with complex subsurface environments along the plane of the profile. Resistivities are assumed to be constant in the third dimension perpendicular to the survey line.

Geophysical Borehole Logging

Geophysical logs have been used for decades to characterize lithology, permeability, and flow conditions in boreholes. The logs used in this study included: caliper, natural gamma ray, spontaneous potential (SP), formation resistivity, water temperature and the heat pulse flow meter (HPFM). The natural gamma ray, spontaneous potential (SP) and formation resistivity measurements are used to determine changes in lithology and/or fluids in the rock adjacent to the borehole. The formation resistivity log is used as an independent test to verify the subsurface resistivities measured with the surface resistivity profiles. The caliper measures variations in the borehole size and locates weathered zones or open fractures associated with flowing waters.

Water temperature and HPFM logs were run before pumping (ambient conditions) and after limited pumping of the well. The water temperature logs from ambient and pumping conditions can indicate where flowing fractures exist by identifying waters of different temperature signatures as fracture water flows into the borehole with a different water temperature. Comparing before-pumping and after-pumping water temperature logs over short depth intervals can indicate specific depth zones where water from fractured aquifers is introduced to the borehole. The HPFM is used to detect the direction and magnitude of vertical flow within a borehole and measures flows over the range of 0.04 to 10 liters per minute. The HPFM has an electrified wire mesh that heats a small quantity of vertically flowing water in the borehole as the water moves through a measurement chamber in the tool. The elapsed time for the heated water to arrive at a thermistor located 2 cm above or beneath the heated wire mesh is measured, allowing calculation of the vertical flow rate in the borehole. The tool is positioned at specific depth intervals and held motionless while the flow measurements are made. Multiple flow measurements are logged versus borehole depth allowing analysis of the flow conditions in the borehole. HPFM measurements are usually first made under ambient conditions and then again during pumping of the well being tested by the HPFM or by pumping a different, but structurally connected, well in the area. Changing the head in a borehole via pumping allows the HPFM to quantify the flow from each fracture that contributes to the overall yield of a well. In this way, several hydrogeologic scenarios can be tested using the HPFM in conjunction with pump testing of specific intervals (Paillet, et. al., 1996).

AQUIFER SYSTEM ANALYSIS

Eight surface geophysical profiles and nine boreholes were examined to determine the character of the shallow and deep aquifers in the field site. Figure 1.5 illustrates the locations of the resistivity lines and observation wells that correspond to the resistivity profiles in subsequent discussions and illustrations.

Shallow stratigraphy in the regolith

The regolith is composed of soil and saprolite with significant variability in the quantity of clay and coarser unconsolidated materials. The upper 20 m of resistivity profile 8 (Fig. 1.6) illustrates some of the variation in the shallow stratigraphy in the regolith. This resistivity profile characterizes the regolith as having: 1) a discontinuous shallow layer extending approximately 0 to 10 m below the surface and consisting of intermediate-to-high resistivities ranging from 900 to 9000 Ω-m and, 2) a deeper layer extending approximately 10 to 20 m below the surface with low to intermediate resistivities from 250 to 1250 Ω-m. Cuttings from boreholes were used identify the lithologies present in the regolith. The shallowest layer is a thin (< 1 m) soil interval at the surface. Saprolite with scattered quartz cobbles is prevalent beneath the soil and extends downward through this interval. The saprolite is composed of micaceous sand and clay and often appears to be very dry. The dry saprolite corresponds to the high resistivity (2000-9000 Ω-m) measurements in the profiles. Lower resistivities (900-2000 Ω-m) are indicative of somewhat higher moisture content (but unsaturated) saprolite in this interval. Layered shallow unsaturated intervals exhibiting high and intermediate resistivities and shallow localized intermediate and low resistivity zones as seen in profile 8 (Fig. 1.6) are common in the field site and have been observed elsewhere in the Blue Ridge and Piedmont provinces by these authors. The presence of both high and low resistivity intervals locally in the shallow subsurface at various topographic settings infers that downward vertical percolation of precipitation in the regolith may be

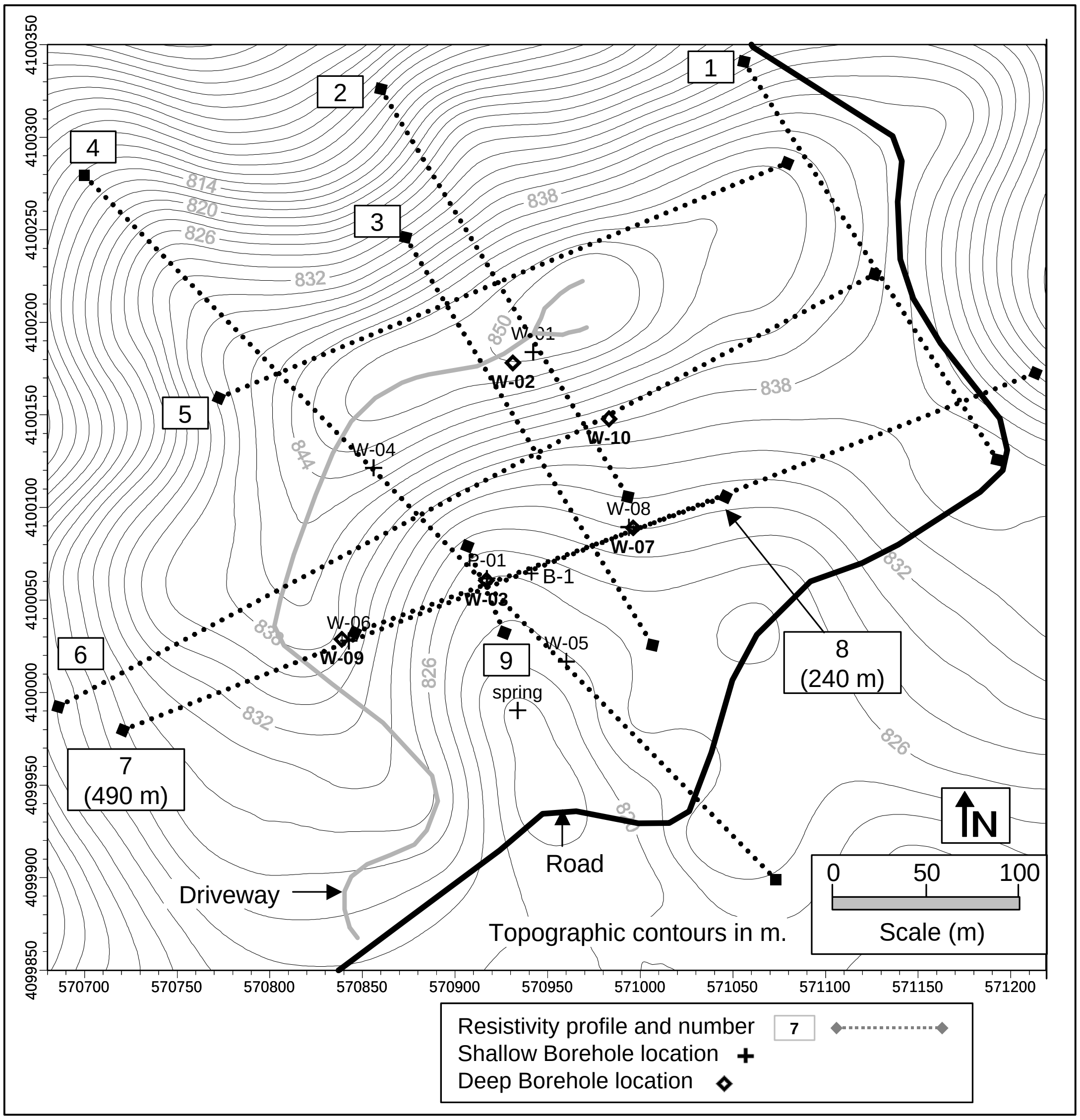

Figure 1.5 Base map of the field site in the Check Quadrangle, Floyd County, Virginia. Borehole and resistivity profile locations shown on topographic contours.

controlled by variations in the subsurface geology rather than changes in rainfall. The dry saprolitic layer associated with high resistivity measurements may indicate relatively impermeable conditions whereas the lower resistivity intervals may represent permeable regolith where precipitation can enter and recharge the regolith and bedrock aquifers.

In the vicinity of borehole 3 on profile 8 is a shallow low resistivity zone (300-600 Ω-m) associated with localized, saturated, sand and clay layers. This shallow low resistivity zone can be seen on Profile 9 (Fig. 1.7) as it intersects profile 8 at the location of borehole 3. The caliper

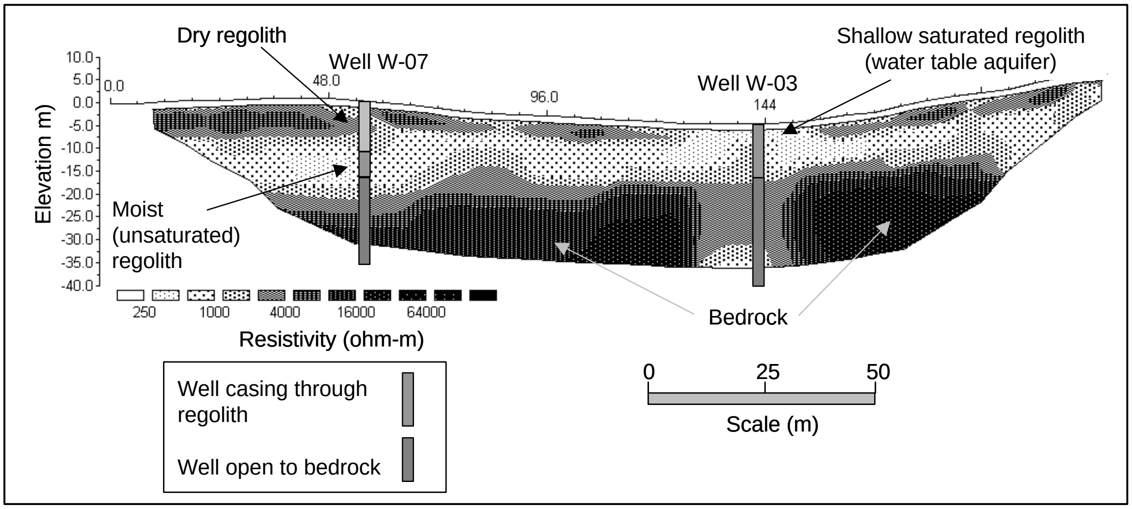

Figure 1.6 Resistivity profile 8 showing shallow regolith and bedrock intervals. Layered high and intermediate resistivities (dry regolith) adjacent to low resistivity intervals (saturated water table aquifer) are illustrated in the shallow aquifer.

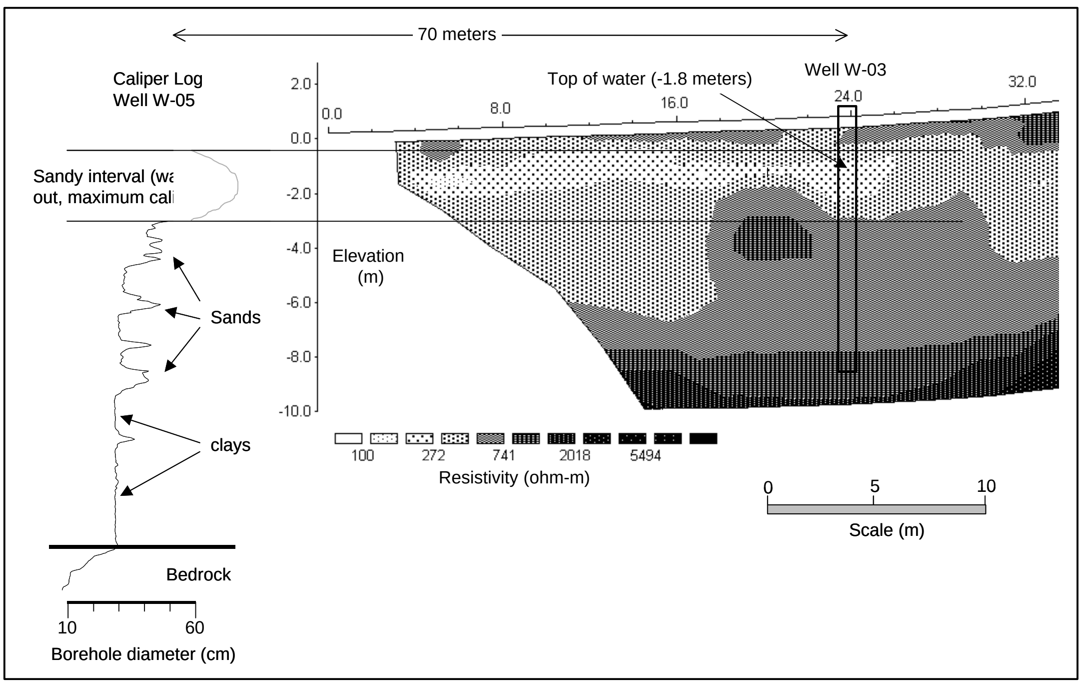

Figure 1.7 Resistivity profile 9 illustrating shallow sandy interval and water table aquifer. Well W-05 caliper log reveals a shallow, washed-out sandy layer above a more clay-rich interval.

log from borehole 5 is correlated with the low resistivity zone in profile 9 and illustrates the sand and clay layers present in this interval. Profile 9 indicates that the shallow sandy interval is 0.3-

1.5 m thick, is localized around the vicinity of borehole 3, and is relatively horizontal. Water table conditions were encountered 1.8 m below the surface in borehole 3 correlating the shallow low resistivity layer with saturated regolith. In borehole 5 (south of profile 9) the shallow sandy interval is 2.3 m thick and unsaturated indicating that a permeability barrier exists between boreholes 3 and 5 in the shallow sandy interval. The water table aquifer in profiles 8 and 9 is also bounded to the northeast and southwest by clay-rich regolith. In Figure 1.8, borehole B-1 is located within the dry high resistivity shallow zone adjacent to the low resistivity saturated interval in Well W-03.

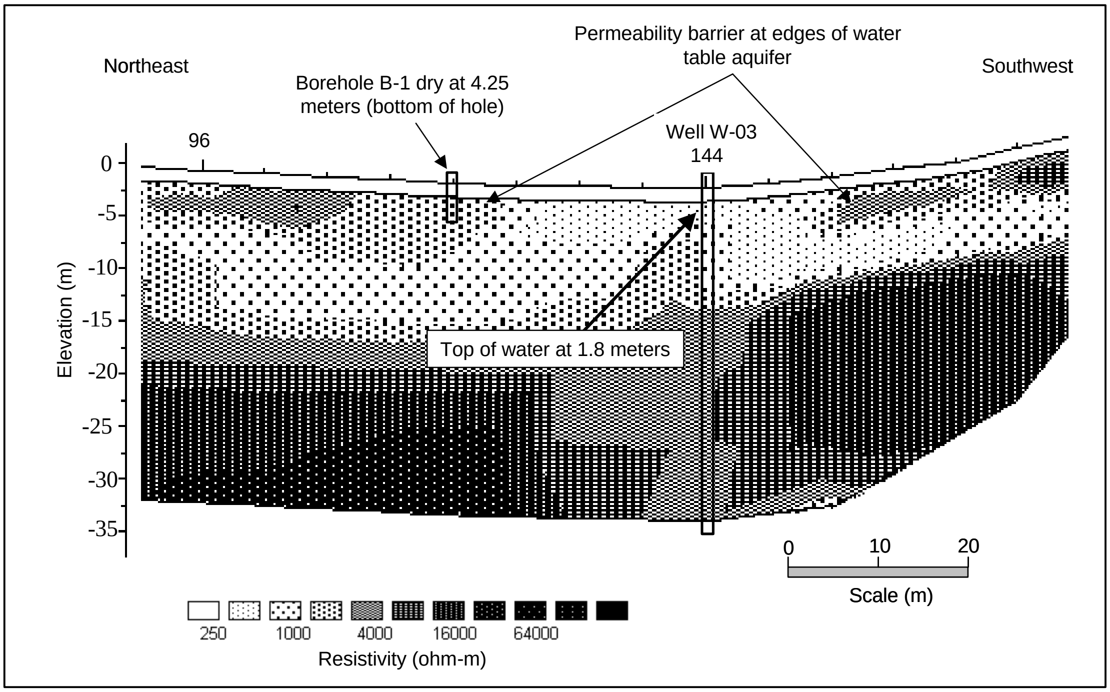

Figure 1.8 Resistivity profile 8 illustrating the permeability barrier surrounding the shallow water table aquifer. Well W-03 encountered saturated sands in the same interval that borehole B-1 found dry, clay rich saprolite.

The resistivity profiles clearly discriminate between dry and saturated conditions in the shallow part of the regolith and also illustrate the complex stratigraphic relationships that exist in this interval. The deeper layer within the saprolite contains moist unsaturated micaceous sand and clay. Variations in resistivity in this interval may be due to changes in moisture content, amount of clay, degree of weathering, or the presence of large pieces of bedrock “float” in the regolith. A saturated transition zone may be present in the base of the regolith, lying directly on top of the bedrock. The transition zone or “first water” in driller’s terminology is relatively thin (~1 m) and has been reported to have high transmissivities relative to the other aquifers in the regolith (Daniel, 1996). The resistivity profiles indicate an increase in resistivity over the depth interval containing the regolith-bedrock interface. The thin transition zone on top of the bedrock is not resolved as a separate interval on the resistivity profiles, however the thickness of the resistivity transition from the lower regolith (250-1250 Ω-m) to bedrock (>1250 Ω-m) can vary from 0 to 10 m. This suggests that the high resistivities associated with the top of bedrock are being lowered by the overlying saturated transition zone or by weathering of bedrock at the top of the regolith-bedrock interface.

The highly heterogeneous nature of the regolith observable in the boreholes and resistivity profiles and the presence of both confined and unconfined aquifers above the fractured bedrock are contrary to the simple single-layer water table aquifer model currently used to characterize this interval. The complexity in the shallow regolith aquifers will directly influence the nature of recharge into, and flow through, the deeper fractured bedrock aquifers.

Analysis of Bedrock Lithology and Structure

Eight long resistivity profiles were collected over the field site with the goal of imaging the regolith and bedrock intervals (Figs. 1.9 a-b). Bedrock resistivity patterns detected in the profiles vary considerably from fairly homogeneous high resistivity zones greater than 4000 Ω-m to discontinuous high and lower resistivity areas elongated both vertically and horizontally. Profiles 1 to 7 range in length from 240-480 m with maximum depths from 50 to 110 m.

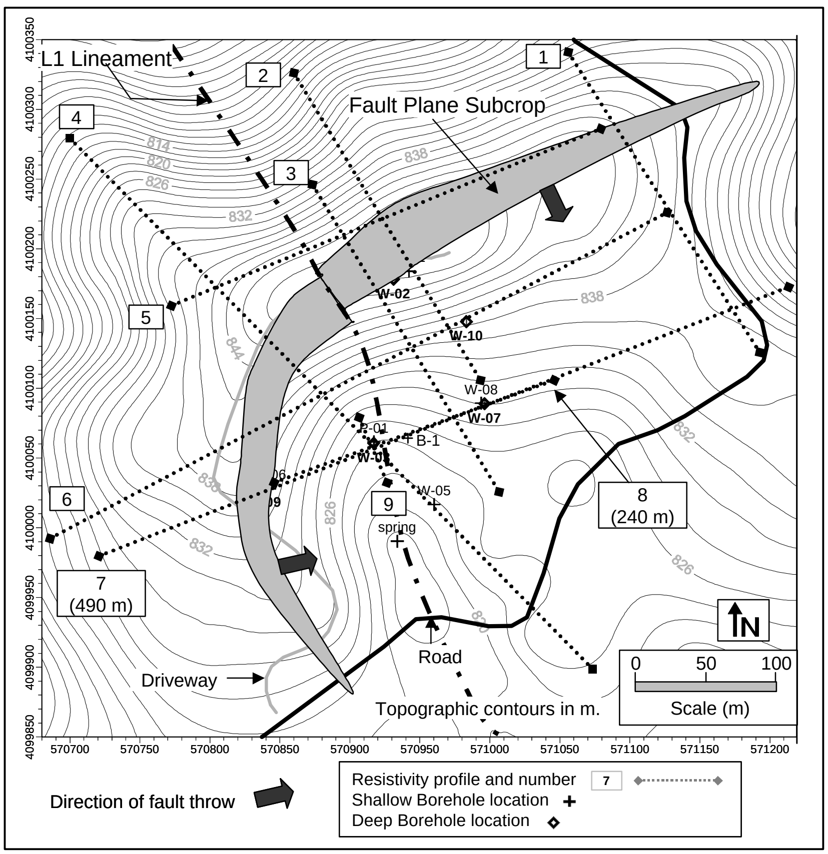

Figure 1.9 (a) Basemap of the field site with arcuate subcrop of the relatively low resistivity east and southeast dipping thrust fault.

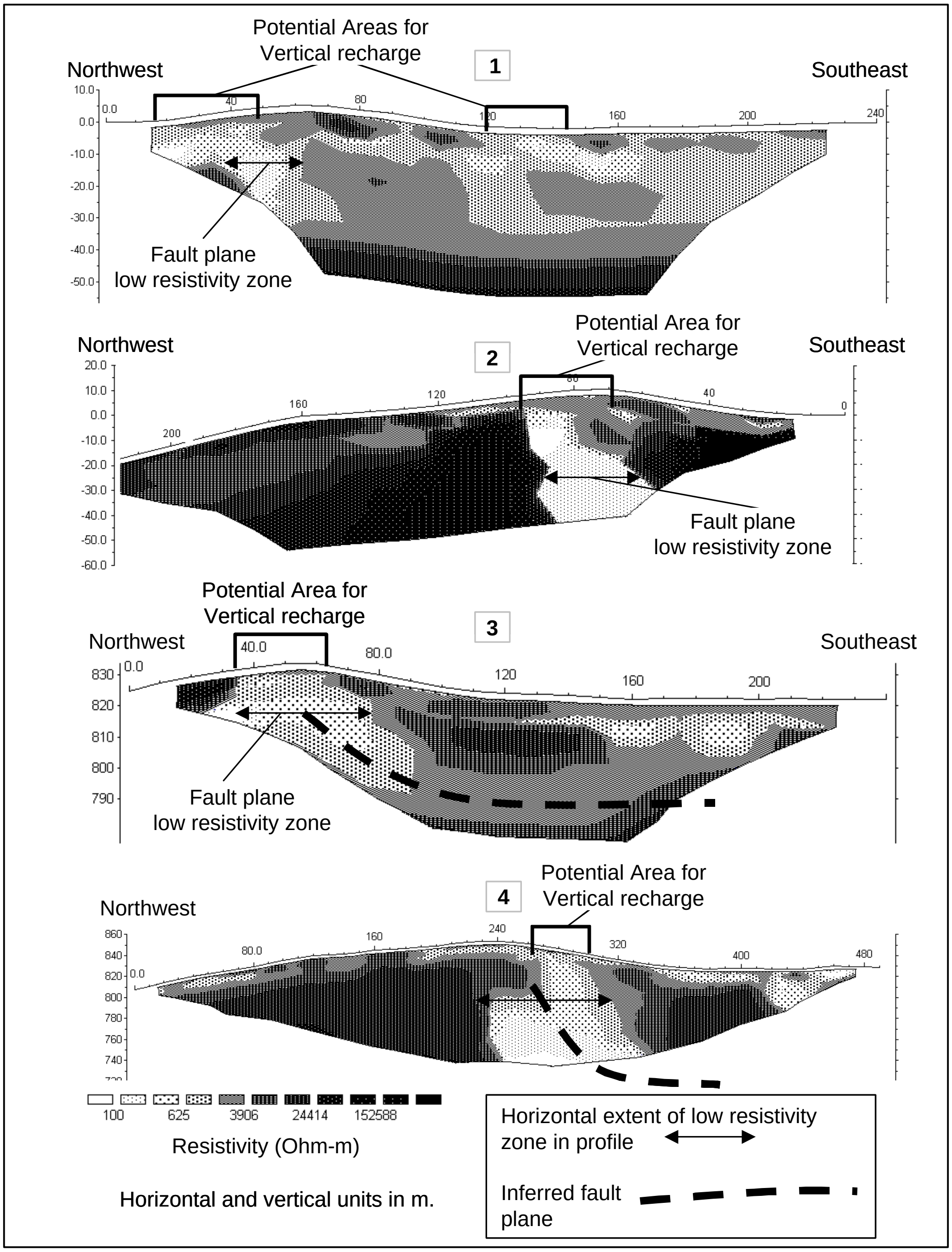

Figure 1.9 a Resistivity profiles 1-4 illustrating regolith, bedrock, and relatively low resistivity thrust fault.

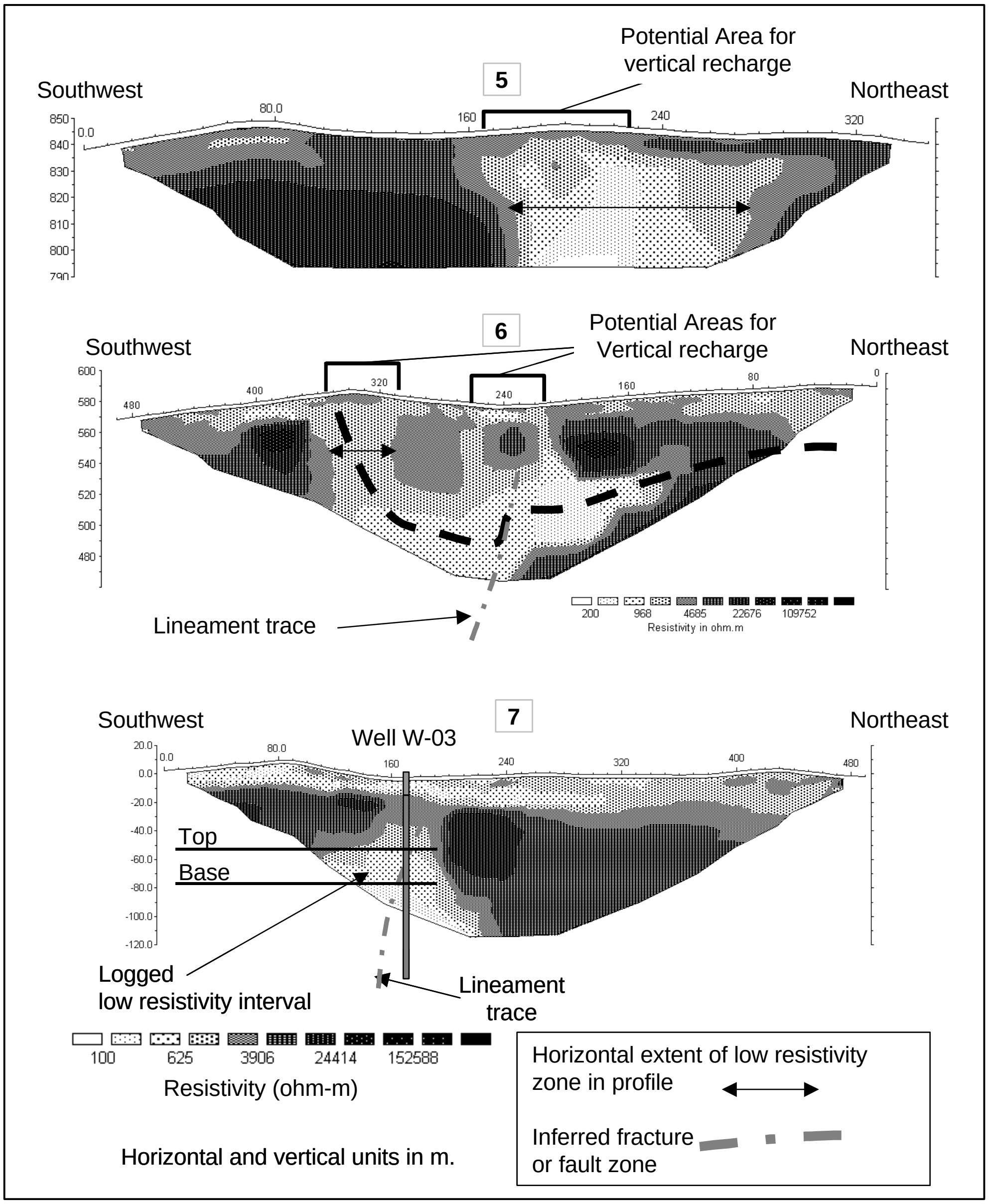

Figure 1.9 b Resistivity profiles 5-7 illustrating regolith, bedrock, and relatively low resistivity fracture and fault zone.

Profiles 1 to 6 document a high angle lower resistivity zone that correlates to the sliding surface (fault plane) of a thrust fault that bisects the field site. Profiles 1 to 4 and profile 6 are perpendicular to this fault plane, profile 5 is tangent to the northwest side of the fault. Profile 6 cuts along the strike of the fault plane in the subsurface. The lithology of the fault plane zone is gray-green mica-schist that weathers brown in outcrop. The resistivity profiles indicate that the fault plane is a low resistivity zone (150-1000 Ω-m) that extends into the bedrock interval. The fault plane intersects the ground surface at a high angle and then appears to become more horizontal towards the southeast as it extends into the subsurface (profiles 1, 3, 4, 6). The fault plane's proximity to the surface and the low resistivity zones in the regolith adjacent to the fault planes suggest that recharge from precipitation is occurring to the regolith and bedrock aquifers at the updip limit of these faults along the crest of the ridge. The arcuate pattern in map view (Fig. 1.9a) is a low resistivity zone that reveals the surface expression of the high-angle thrust fault subcrop. The spatial distribution of similar ridges in the vicinity of the field site outlines the northwest extent of a series of thrust sheets associated with Paleozoic tectonism (Fig. 1.10). Each of these ridges may be separate areas for precipitation to enter the subsurface and recharge the underlying regolith and bedrock aquifers.

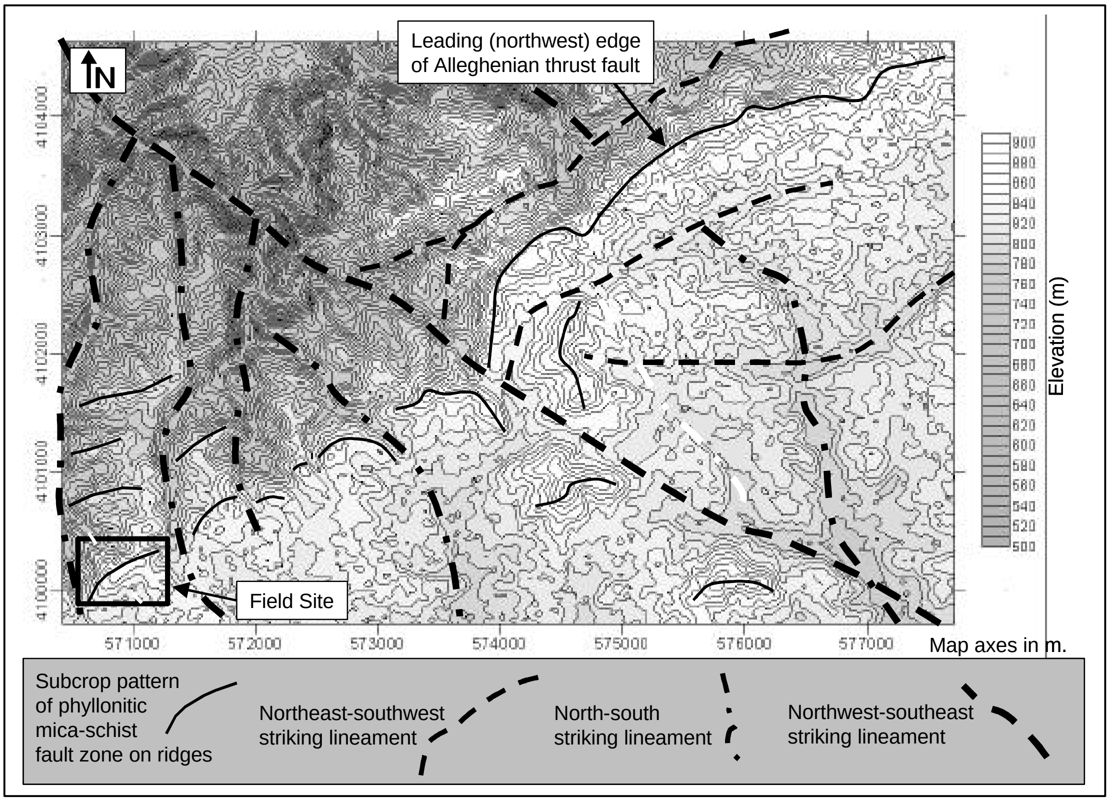

Figure 1.10 The spatial distribution of ridges in the vicinity of the study area outlining the northwest extent of a large thrust sheet associated with Alleghenian (late Paleozoic) deformation. Some offsets are Mesozoic or younger (Walsh-Stovall, et al., 2000).

A northwest-southeast oriented lineament (L1) with surface topographic expression is located in the center of the field site (Fig. 1.9a). Lineament L1 intercepts the fault plane seen in the resistivity profiles and is imaged by profiles 6 and 7. This lineament is also associated with a vertical, relatively low resistivity zone in profile 7. This low resistivity zone is approximately 100 m wide and extends deep into the subsurface below the bottom of the profile.

Borehole geophysical logs for well 3 confirm the presence of a thick, relatively low resistivity interval in the subsurface (Fig. 1.11). The low resistivity zone measured with the borehole resistivity tool (44 to 66 m depth) corresponds with the low resistivity zone in the surface resistivity profiles 4 and 7 (Figs. 1.9 b,c). The average resistivity of the low resistivity interval between 44 and 66 m depth in the borehole log is 1780 Ω-m. The crystalline bedrock above the logged low resistivity zone averages 4770 Ω-m, and the bedrock below it averages 5470 Ω-m. Profile 7 indicates a relatively low resistivity zone beginning from 46.5 m depth to the bottom of the section (>90 m) at the location of borehole 3. The low resistivity zone in the profile ranges from 625-1562 Ω-m.

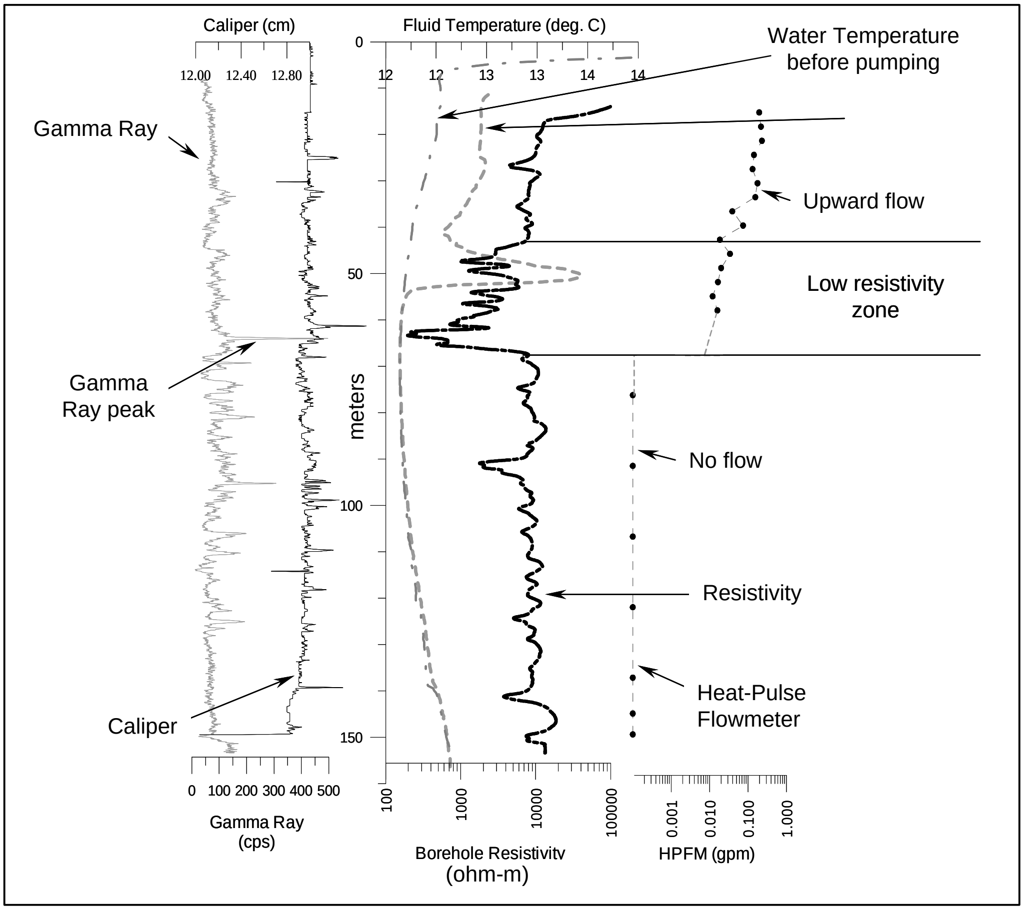

Figure 1.11 Well W-03 borehole geophysical logs. Low resistivity zone in W-03 correlates with low resistivity interval on resistivity profiles. Upward flow in W-03 begins in the low resistivity interval (45-65 m depth).

The presence of the low resistivity zone in the profile below the zone indicated by the borehole logs may be due to the several factors. The profile may be imaging low resistivities associated with an interval proximal to the plane of the section but distant from the borehole.

Because resistivity profiles are 2-dimensional, they assume constant resistivities perpendicular to the line of the profile. Significant horizontal variation in lithology exists in this area as evidenced by the differences in resistivity between profiles 6 and 7; this possibly causes the resistivity differences between the deeper part of the profile and the borehole log. A full 3 dimensional resistivity survey utilizing resistivity borehole tomography could solve this problem. Another possible explanation for the discrepancy may be due to a lack of sensitivity of the dipole-dipole array at these depths that would allow the inversion process to assign a wide variety of resistivities to the deep part of the profile (see Appendix A for dipole-dipole array geometry). Using borehole resistivity tomography or a 3 dimensional surface resistivity array would minimize this problem.

Fracture location and flow rates in borehole 3 were determined using the fluid temperature and HPFM tools respectively. Fluid temperature logs were obtained from trolling the probe down the borehole under ambient conditions. While the fluid temperature tool was at the bottom of the well, pumping was commenced. The pumping rate was set to lower the water level approximately 6 m and then maintain that level of drawdown while a second temperature log was obtained by trolling the probe up the borehole. Visual inspection of the temperature logs obtained under ambient and pumping conditions reveal the depth intervals of flowing fractures. The temperature logs in Fig. 1.11 indicate significant temperature contrasts in the interval from 10 to 53 m, with the most pronounced temperature anomaly at the top of the low resistivity zone between 40 and 53 m. This temperature anomaly is associated with highly fractured granulite gneiss that has been logged in outcrops at the top of the mylonitic mica-schist intervals by Henika (VDMR, personal commun. 1999) and Bartholomew, et al, (1999). This fractured granulite gneiss is associated with the fault plane and represents a zone of intense fracturing; the degree of brecciation appears to be directly associated with the proximity to the fault plane. The HPFM data corroborate these field observations. Well bore flow measured with the HPFM indicates that the deepest and most active flow occurs near the base of the low resistivity zone (approximately 60 m depth), with additional inflows occurring upward through the granulite gneiss facies. HPFM data do not indicate measurable flow in the well bore below the low resistivity zone (below the mica-schist representing the fault plane). The warmer waters associated with the temperature anomaly from 40-53 m depth may be flowing from shallower depths whereas the waters below the temperature anomaly may originate from fractures in a deeper bedrock interval.

The relatively low resistivity zones associated with vertical lineaments and the thrust fault planes are due to the presence of thick intervals of steeply-dipping mylonitic mica-schist. This mica-schist formed during the shearing action responsible for these faults and the subsequent metamorphism that occurred after deep burial of these rocks. Brecciated gneiss has been noted at the top of the thrust fault shear zones. Brecciated gneiss is responsible for the high hydraulic conductivity and increased flow measured in well 3 at the top of the low resistivity zone. Near the base of the low resistivity fault shear zone, at approximately 65 m depth, is a thin high gamma ray “spike” indicates the presence of concentrated radioactive materials. Thin radioactive zones similar to this interval commonly occur at the base of fault planes in the Blue Ridge province and other areas (W.S. Henika, personal commun. 1999) and are likely associated with the presence of concentrated potassium isotopes.

CONCLUSIONS

Integration of geophysical data from surface resistivity profiles and borehole logs with geologic data from borehole cuttings, outcrops, surface lineament studies and well drilling data at a field site in Floyd County, Virginia, has provided new insights into the nature of the aquifers in the regolith and crystalline bedrock in the Blue Ridge Province.

Surface resistivity profiles reveal significant variations in subsurface resistivity within the shallow regolith and deeper bedrock intervals. The differences in resistivity are associated with lithologic changes and variations in water saturation. The regolith in the Blue Ridge Province has been previously described as a simple unconsolidated interval of soil and weathered rock containing a water table aquifer supplying water to the underlying fractured bedrock at a relatively uniform rate. This study reveals relatively complex stratigraphy composed of sand and clay prone intervals, a localized water table, and extensive, thin, confined aquifers in the regolith. Large portions of the regolith are unsaturated and may not be serving as pathways for vertical recharge of the bedrock aquifers.

The crystalline bedrock also was determined to have a more complex hydrogeology than previously described. Current models of the Blue Ridge hydrogeology generally rely on permeable fracture sets associated with late tectonism in otherwise homogeneous and impervious bedrock to serve as conduits for groundwater flow. This study revealed hydrologically significant lithologic variation in the bedrock and fault shear zones that can act as pathways for recharge and subsurface flow. Shear zones resulted from the heat and abrasion that occurred on the sliding surfaces of faults that were active during the mountain building episodes of the Blue Ridge Province. Above the shear zones are intervals of fractured granulite gneiss, caused by the faulting, that can act as high hydraulic conductivity pathways for groundwater flow. Extensive fracture zones may connect the upgradient recharge areas at the surface with the subsurface flow seen in deep bedrock fractures. These ancient fault zones can be imaged with borehole and surface resistivity techniques providing an indirect and non-invasive method to study the fractured aquifers.

By locating the recharge areas and flow pathways within crystalline rocks, reasonable conclusions regarding groundwater movement for water supply, contaminant transport and watershed/wellhead protection issues. This study is part of an ongoing investigation of the groundwater hydrology of the field site described herein. Extended aquifer tests, detailed water level measurements and additional geophysical logging are planned to verify and quantify the subsurface conditions described in this paper.

Chapter 2: Aquifer Test Analysis and Aquifer Characterization in the Blue Ridge Physiographic Province

ABSTRACT

Existing models of the hydrogeology in the Blue Ridge and Piedmont provinces in the eastern United States generally assume a simplified two-layered system consisting of shallow unconsolidated and relatively homogeneous and porous regolith with a water-table aquifer that slowly supplies water downward to the underlying variably fractured crystalline bedrock. In these models, interconnected fractures in the crystalline bedrock act as conduits for predominantly downward vertical and limited horizontal flow. Fracture density is depth–limited and correlated with proximity to topographic lineaments. Current models consider the porous regolith as the primary water storage reservoir for the entire aquifer system.

In this research, detailed hydrogeologic studies in the Blue Ridge Province in Floyd County, Virginia reveal a substantially different framework for groundwater flow. The shallow aquifer occurring within the saprolite and the top of the bedrock is often separated from the underlying fractured bedrock aquifer by an aquitard. Hydraulic heads between the shallow aquifer and the deeper bedrock fractured aquifer can vary by 20 m vertically. Both of these aquifers are commonly encountered under confined aquifer conditions. High fracture density within the bedrock can be correlated with ancient fault shear zones that originated from thrust faulting. Brecciated rock adjacent to the shear zones, and fractures that intersect the shear zones, can have high hydraulic conductivities.

Aquifer testing of the regolith-bedrock fracture system occurred over a 6-day period and produced rapid and relatively uniform drawdowns in surrounding wells completed in the fractured bedrock aquifers. This information combined with geophysical logging data indicates that horizontal flow is predominant in the bedrock fractures. The shallow regolith aquifers experienced minimal drawdowns from the aquifer test indicating low vertical hydraulic conductivity and limited communication between the shallow and deeper bedrock aquifers. Recharge of the fractured aquifers may be occurring in localized areas where significant hydraulic communication exists between water sources at the surface or in the regolith and the underlying fractured bedrock. Water chemistry and chlorofluorocarbon (CFC) age dating analyses showed significant differences between water samples from the shallow and deep aquifers. A new conceptual model for Blue Ridge aquifers is proposed based on this new information.

INTRODUCTION

The Blue Ridge Physiographic Province was formed by the repeated compressional and extensional tectonism that occurred from Precambrian through late Mesozoic-early Cenozoic time. The Blue Ridge metamorphic rocks in Floyd County are within a system of generally northeast striking thrust faults stacked vertically and shingled laterally. The oldest thrust sheets have undergone multiple periods of deformation throughout the Paleozoic and have been crosscut by younger thrust faults. This style of faulting is predominant in the Blue Ridge and Piedmont provinces throughout the eastern United States (Henika, personal commun., VDMR, 2002, Lampshire, et al., 1994, Costain, et al, 1989, Pratt, et al., 1988,). The Blue Ridge Fault (figs. 1.1 and 1.2) underlies Floyd County and is the master decollmont separating the Precambrian metamorphic rocks of the Blue Ridge Province from the Paleozoic age sedimentary rocks below it (Henika, 2000, Walsh-Stovall, et al, 2000). In addition to the generally horizontal thrust faults are numerous near vertical, predominantly north-south and northwest-southeast oriented joints formed during the latest stages of Appalachian tectonism expressed as lineaments in the surface topography (Bartholomew and others, 1999, Henika, personal commun., VDMR, 1999). Bedrock is composed of layered Precambrian granulite gneiss, granitic gneiss, augen gneiss, massive, highly fractured vein quartz, and phyllonite, Cambrian quartzite and phyllite of the Chilhowie Group, and late Proterozoic and Mesozoic diabase dikes. Bedrock usually strikes northeast and dips to the southeast.

The Blue Ridge Province, although geologically complex, typically is viewed as a somewhat simplistic two-layer aquifer system (as is the Piedmont Province) (LeGrand, 1967, Heath, 1984, and others). This aquifer model assumes a relatively homogeneous unconsolidated layer of soil and weathered rock (saprolite) containing a water table aquifer of high storage capacity supplying water to an underlying variably fractured homogeneous crystalline bedrock aquifer that has low overall porosity and low storage capacity. Interconnected fractures serve as conduits for predominantly downward vertical and limited horizontal flow, and the number of fractures decreases with depth (fig.2.1). Wells in the region are often limited to 100 m depths because of this accepted perception.

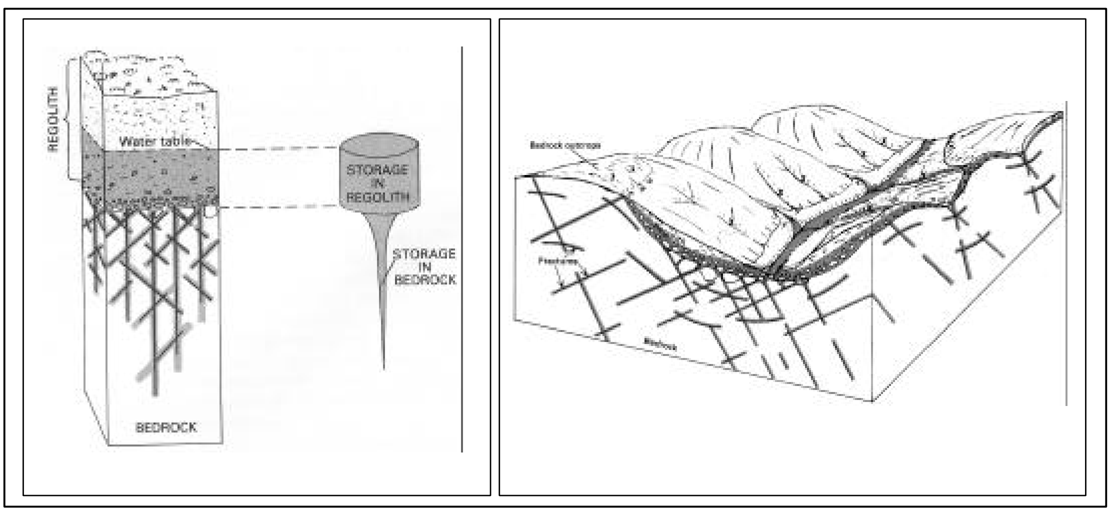

Figure 2.1 Current conceptual model of aquifers in the Blue Ridge and Piedmont provinces (Heath, 1984, LeGrand, 1967) illustrating downward flow from a water table aquifer into underlying fractures.

Research and field observations during the last five years at the Department of Geological Sciences at Virginia Tech and by others in the Blue Ridge and Piedmont provinces in Virginia and North Carolina have often been at variance with the conceptualization described above. A groundwater research field site located 30 kilometers southwest of Roanoke, Virginia, near the western edge of the Blue Ridge Province in Floyd County, Virginia has been established to investigate the character of the aquifers in this region (fig. 2.2). The field site contains numerous bedrock outcrops, springs, and 11 boreholes varying from 10 to 300 m depth. Seaton and Burbey (2000) described the geologic framework of Blue Ridge aquifers at the field site and proposed addition aquifer tests to substantiate their findings. This research presents the latest aquifer-test results, water-chemistry analysis including groundwater age dating, and proposes a new conceptual model of the flow system in the Blue Ridge Province.

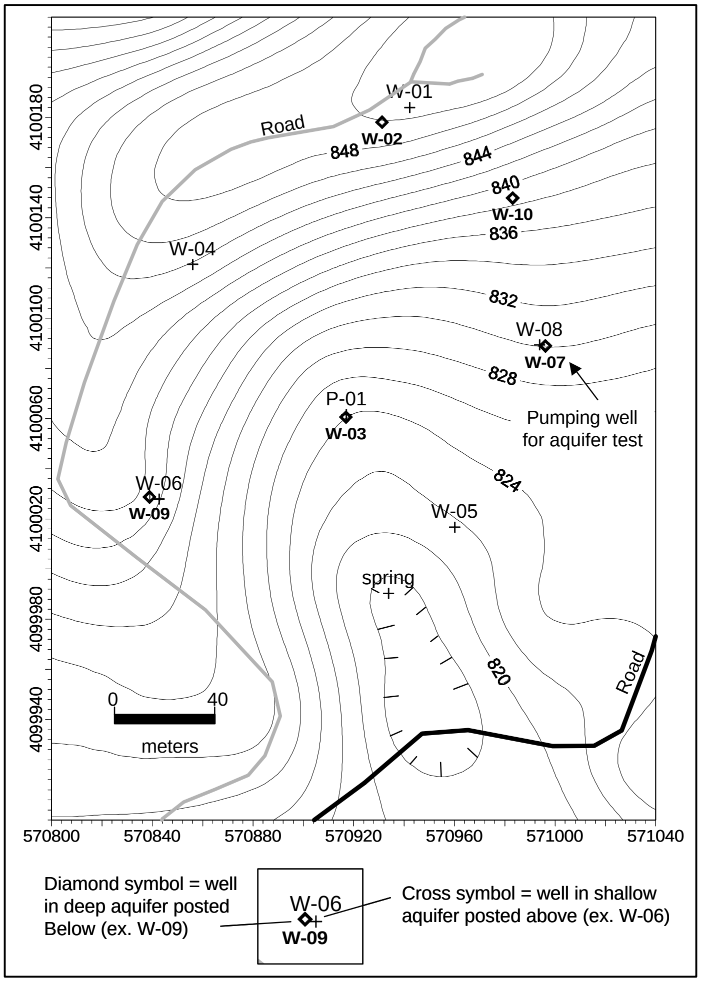

Figure 2.2 Field site with topographic contours in meters, locations of shallow and deep wells, and spring.

DATA COLLECTION AND ANALYSIS PRIOR TO AQUIFER TESTING

The initial hydrogeological characterization of the site was based on surface and borehole geophysics, water level measurements, and geological data collected from outcrops and boreholes. Numerous two-dimensional surface resistivity profiles were collected throughout the field site revealing the subsurface electrical resistivity distribution to approximately 100 m depth (Seaton and Burbey, 2000). Two-dimensional surface resistivity profiling accounts for the spatial variation in earth resistivities associated with complex subsurface environments along the plane of the profile. These profiles delineated saturated and unsaturated areas in the shallow unconsolidated saprolite and also allowed for the identification of massive bedrock from fault zones. Fault zones with high hydraulic conductivity are often associated with phyllonite and fractured granulite gneiss. In addition to the resistivity surveys, borehole geophysical logs were collected at 8 of the 11 wells at the site. Borehole data were collected using the caliper, natural gamma ray, spontaneous potential (SP), formation resistivity, water temperature and heat pulse flow meter (HPFM) probes. These tools were used to characterize the subsurface geology and hydrogeologic conditions prior to the aquifer test described here (Seaton and Burbey, 2000). Appendix D illustrates the key borehole data from the logged wells.

Use of these geophysical data along with hydrogeologic mapping indicates that the zone between the regional thrust faults presented in figures 1.1 and 1.2 represents a duplex thrust fault system. Phyllonite sequences observed as mica schists in outcrop represent the rock unit associated with ductile deformation during active thrusting during late Paleozoic time (W. Henika, VDMR, personal communication, 1999). The adjacent overlying granulite gneisses became highly fractured above the ductile deformation zones. These intensely fractured granulites now include highly permeable fault zones (Walsh-Stovall, et al, 2000), whereas the mica schists may now form a generally impermeable lower unit and a ramp for deep groundwater flow above this fault plane. This region of high permeability can manifest locally as a zone 10 m in thickness or as a single 0.3 m width fracture. The thrust fault is expressed at the ground surface as a northeast-southwest trending arcuate ridge that is part of a series of similar ridges along the strike of a semi-regional thrust fault system. The fault is encountered in the shallow cased portions of wells W-01 and W-02 then dips steeply and becomes semi-horizontal beneath wells W-03 and W-07 at a depth of 45-60 m below land surface (fig. 2.3). The regional fracture and lineament sets associated with tensional forces are also imprinted on the bedrock.

Several deep wells penetrate the aquifer associated with the fractured bedrock (termed “deep aquifer”), while others are open only within the unconsolidated saprolite or penetrate very shallow bedrock (termed “shallow aquifer”). Hydraulic-head differences between wells completed in the shallow and deep aquifer are variable. Along the crest and adjacent slope of the northeast-southwest trending hill, heads within the shallow aquifer are higher than the water levels in the deep aquifer. The difference in head values decreases to the south and southwest (fig. 2.4). Near a spring at the field site the head differences are minimal. Single-well borehole testing and contouring of water levels indicate that relatively impermeable bedrock is acting as an aquitard separating the shallow and deep aquifers (fig. 2.5a-c).

AQUIFER TEST ANALYSIS

Well W-07 was used as the pumping well during the nearly six-day aquifer test conducted in late spring of 2001. W-07 has the highest yield of all wells on the site and is completed only in the deep aquifer. Pressure transducers were installed in each well to monitor

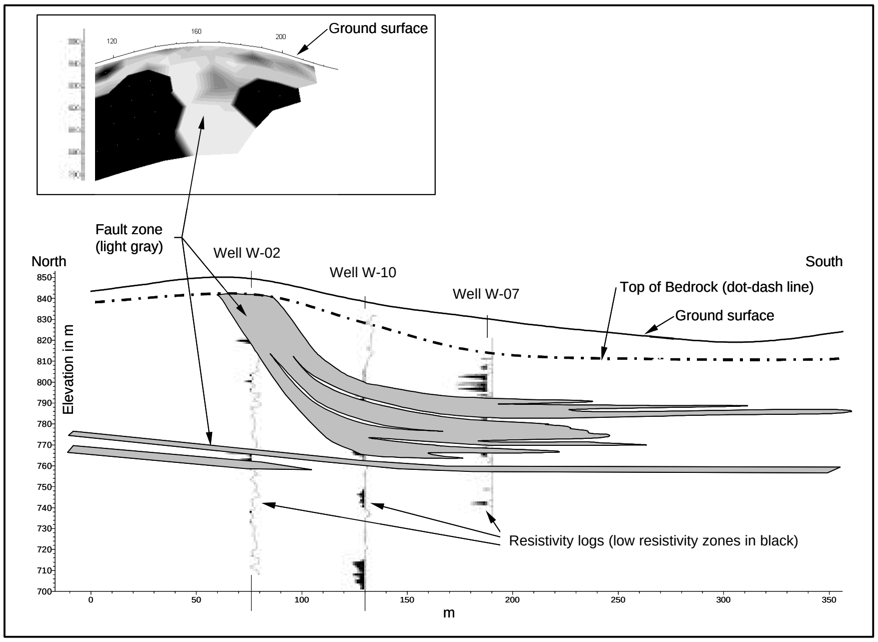

Figure 2.3 Geologic cross section through wells W-02, W-10, and W-07. The fault zone is indicated in light gray in the cross section. The black zones in the well logs are low resistivity intervals corresponding to the fault zone. The resistivity profile at the top shows a near vertical, low resistivity, fault zone (light gray), high resistivity granulite gneiss (black), and shallow saprolite adjacent to the ground surface (light-dark gray) in the vicinity of the northern part of the cross section.

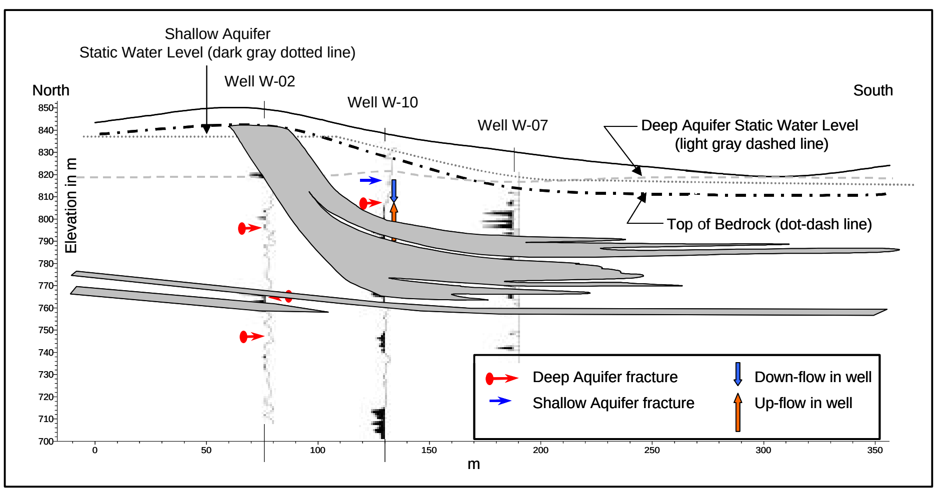

Figure 2.4 Geologic cross section through wells W-02, W-10, and W-07 illustrating static water levels and fracture zones from shallow and deep aquifers. Downflow from shallow aquifer and upflow from deep aquifer indicated in Well W-10.

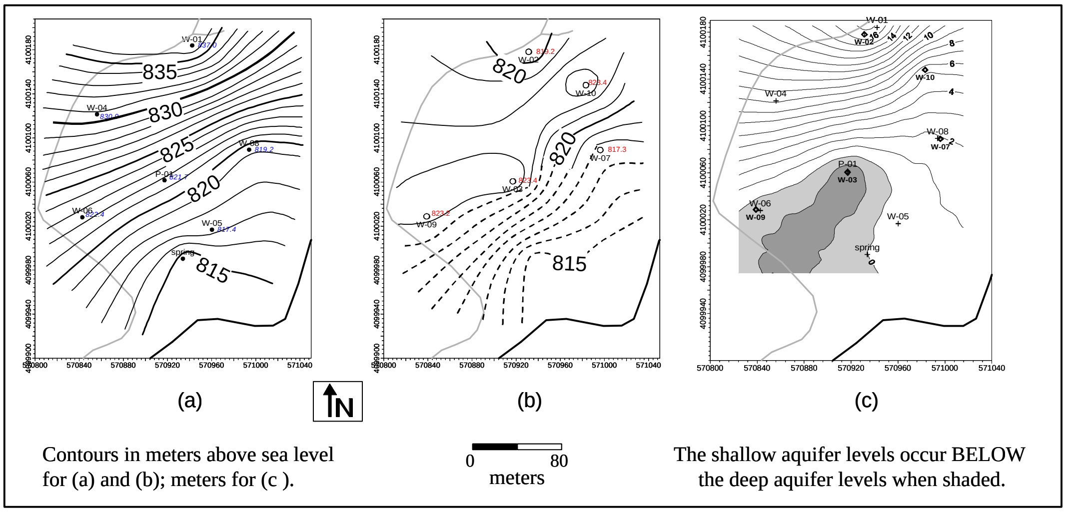

Figure 2.5 Water level contours for the shallow (a) and deep (b) aquifers. Subtracting the deep contoured water levels from the shallow water levels produces (c). Shallow aquifer water level (a) has relatively uniform slope. The deep aquifer has flatter water level contours and occurs above the shallow aquifer in the southwestern part of (c).

water levels prior to, during, and after the six-day test. Wells were not packed off to isolated fractures so borehole storage effects must be taken into account during analyses. The pump installed in W-07 was placed below the open fracture zone. The initial pumping rate was approximately 50 l/min and was gradually reduced during the six-day test to maintain a fairly constant head in the pumping well of about 26 m below pre-pumping levels. The final pumping rate was 21 l/min. A total of just over 171,000 liters of water was pumped at an average rate of nearly 28 l/min over the duration of the test. After the pump was shut off, recovery was monitored in all the wells until water levels asymptotically reached new equilibrium values.

Time-drawdown plots were constructed for wells completed in the shallow and deep aquifers. Drawdown response in all wells open in the deep aquifer responded similarly. Figure 2.7 is an example of the time-drawdown response of the deep aquifer during pumping for well W-03, located 86 m, west-southwest of the pumping well. Early-time response to pumping indicates the time-drawdown plot has a unit linear slope on log-log paper. This response may indicate an extremely transmissive fracture network (Gringarten, 1982) or a transmissive fracture set with significant wellbore storage effects (Kruesman and de Ridder, 1990). After approximately one-half day the plot follows a straight line with a slope of 0.5. The abrupt change is likely due to a lowered pumping rate corresponding to this time; however, the slope also likely represents horizontal parallel flow in a highly transmissive fracture similar to an extended well (Gernand and Heidtman, 1997; Jenkins and Prentice, 1982). Late time response corresponds to a period of pseudo-radial flow, which may indicate contributing flow from lower permeability fractures that intersect the fault zone. The response in wells W-03 and W-10 are nearly identical to the response observed at the pumping well with the exception that their total drawdown is an order of magnitude less than that of the pumping well.

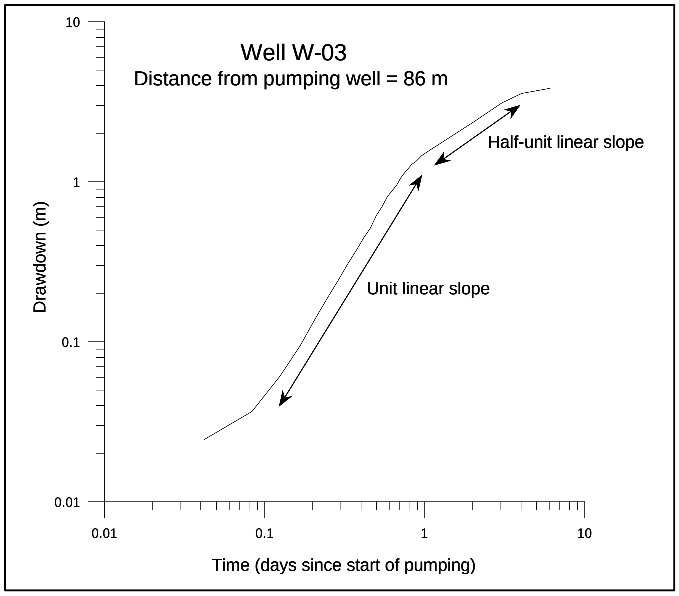

Figure 2.7 Time-drawdown plot for aquifer test, well W-03 (deep aquifer). Unit and half-unit linear slope suggests a highly transmissive fracture network.

Contour maps of the maximum drawdown resulting from the aquifer test (figures 2.8a and 8b) reveal significant differences between the shallow and deep aquifers. The shallow aquifer experienced a maximum of 0.158 m of drawdown in well W-08 with water depth contours elongated toward the southwest.

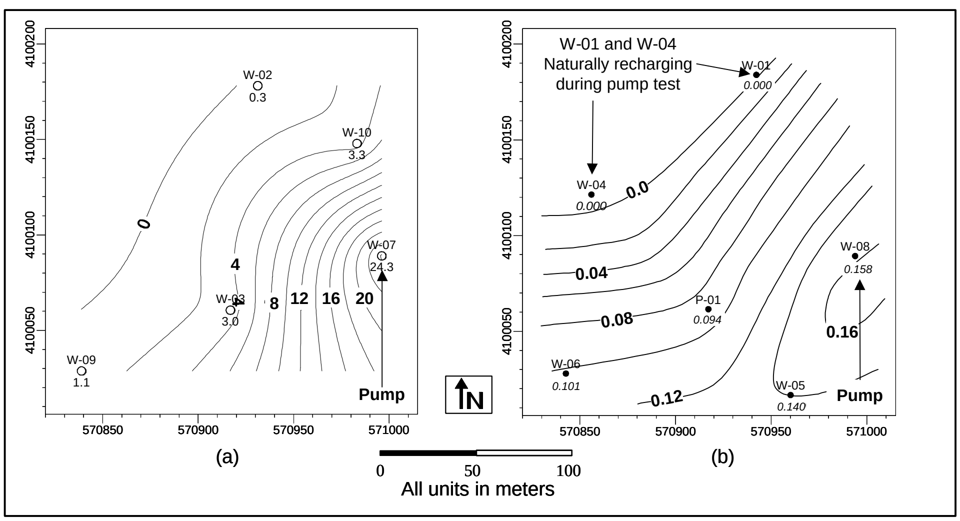

Figure 2.8 Maximum drawdown contours (m) in deep (a) and shallow (b) aquifer resulting from aquifer test.

The most distant wells W-01 and W-04 experienced a small amount of natural recharge during the duration of the aquifer test. The deep aquifer was drawn down 24.3 m at the pumping well (W-07), 3.3 m at W-10, and 3.0 m at W-03 forming a more circular pattern in the drawdown contours. Drawdown was mildly anisotropic (1.5-to-1 ratio) with increased drawdown towards W-10 (north-northwest of pumping well).

The hydraulic conductivity of the flow path from the shallow to the deep aquifer was estimated from time-drawdown plots during pumping by assuming that the vertical distance from the shallow aquifer to the deep aquifer represented the distance to the pumping well. Because the fault zone behaves much like an extended well, this is considered to be a valid assumption. Well W-08 is completed in the shallow aquifer and is located (horizontally) 2.1 m from the pumping well. The actual distance to the pumping well is taken to be 24.4 m in the vertical direction, which is the distance between the shallow aquifer in W-08 and the open fracture zone in W-07. Figure 2.9 documents the results of the aquifer test for W-08. The hydraulic conductivity was estimated for the hydraulic pathway between the shallow and deep aquifers using a Hantush type-curve. Most of the thickness of this section occurs within bedrock, therefore, storage is not considered to be a factor. This pathway slowly contributes water to the deep aquifer and depends on the degree of interconnectivity of the fracture network. Although it is typically perceived that the shallow bedrock in these metamorphic terranes is more permeable than deeper portions of this terrane, this aquifer test clearly indicates otherwise. The estimated hydraulic conductivity of the pathway between the shallow and deep aquifers in this aquifer test is 4.3×10^{-7} m/s or 3.7×10^{-2} m/day, and is approximately six orders of magnitude less than the estimated horizontal hydraulic conductivity of the deep aquifer.

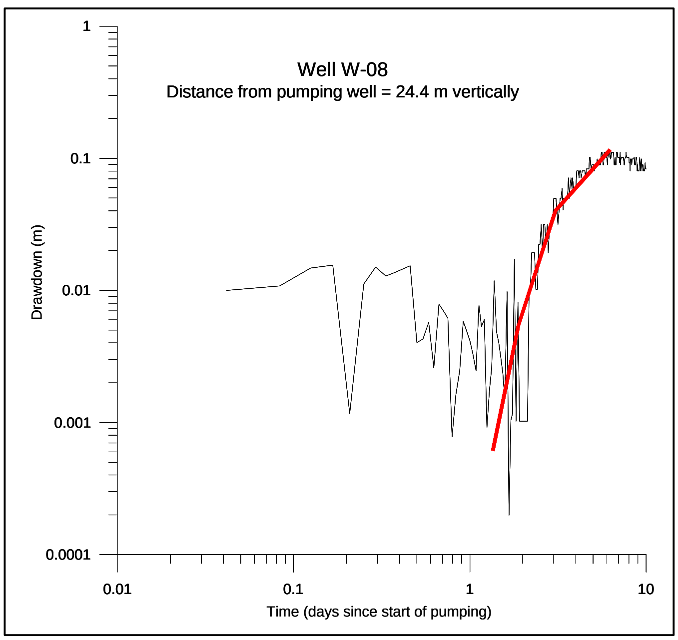

Figure 2.9 Time-drawdown plot during aquifer test for well W-08 (shallow aquifer). Solid line is Hantush type curve for the data.

After approximately six days of continuous pumping the wells were allowed to recover. Recovery tests were performed on all wells. Wells open to both the shallow and deep aquifer experienced immediate response and recovery. However, wells open to the fault-zone aquifer asymptotically approached a new equilibrium head value below that of the pre-pumping static water level. Figure 2.10 illustrates the pumping and recovery data for well W-10 located 63 m from the pumping well and completed in the deep aquifer. Five weeks after the aquifer test the recovery head for W-10 was approximately 1 m below the pre-pumping static head value. Similarly, well W-03, located 86 m from the pumping well, had a recovery head that was approximately 1 m below the pre-pumping static head value after five weeks of recovery. The more distant well 9 (170 m from the pumping well) had a recovery head only 0.25 m below the pre-pumping static head. The recovery in each of these wells was not complete because the volume of water removed during the nearly six-day test lowered the total amount of water in the storage reservoir of the deep aquifer.

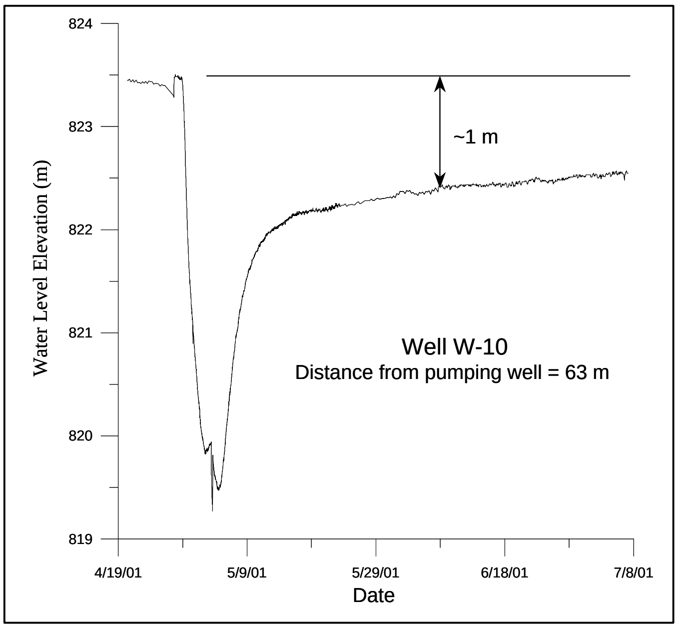

Figure 2.10 Aquifer pumping and recovery test results for well W-10. Recovery data indicates a lowering of the storage reservoir in the deep aquifer due to the aquifer test.

Without directly knowing the porosity or equivalent aquifer thickness from which the water was extracted, it is difficult to project the extent of the radius of influence due to the aquifer test. Heterogeneities in the system and locally non-radial flow conditions also make projecting the size of the reservoir and the distance of pumping influence difficult to estimate. Nonetheless, even with porosities on the order of 0.1 percent, the maximum radial extent that experienced affects of pumping was probably not much more than 300 m. However, the total size of the aquifer or “reservoir” could be considerably larger than the affected radius.

A time-drawdown plot of recovery data after pumping reflected a radial type flow system and suggests that the deep aquifer has a limited amount of water and is ultimately being recharged from the overlying saprolite in localized areas referred to as breach zones or by slow leakage through smaller less permeable interconnected fractures. The time-drawdown recovery data were matched with Hantush leaky type curves that assume no confining-unit storage. Estimated transmissivity values using type-curve matching from recovery data at all wells intersecting the fault zone in the deep aquifer are between 4 and 14 m^2/day. This range signifies the importance of the deep aquifer system as a highly permeable water-producing and storage zone relative to the overlying saprolite aquifer or shallow bedrock.

WATER CHEMISTRY ANALYSIS

Water samples were collected from the shallow and deep aquifers and analyzed for the presence of major anions and cations, metals, dissolved gases, stable isotopes, and CFC's. Samples were collected by members of the USGS Water Resources Division as part of a regional effort to characterize the water chemistry and age of groundwater throughout Virginia (Nelms and Harlow, 2001). Sampling and analysis methodologies are presented in Plummer, et al., (2000) and at the URL:http://water.usgs.gov/lab/cfc. Samples were taken from the shallow aquifer in wells W-01, W-08 and from the deep aquifer in wells W-03 and W-07. Wells W-01 and W-08 are limited to the shallow aquifer; W-03 and W-07 have casing across the shallow aquifer and are only exposed to the deep aquifer. Wells W-03 and W-07 were sampled from two intervals within the deep aquifer. A packer was placed above the high transmissivity fault zone in each well, and samples were taken from the high transmissivity fault zone and from the bedrock interval above this zone. Water chemistry results are from the CFC age dating and the major anion/cation analyses and are presented in figure 2.11 a-c. Other tests did not indicate significant differences between water samples.

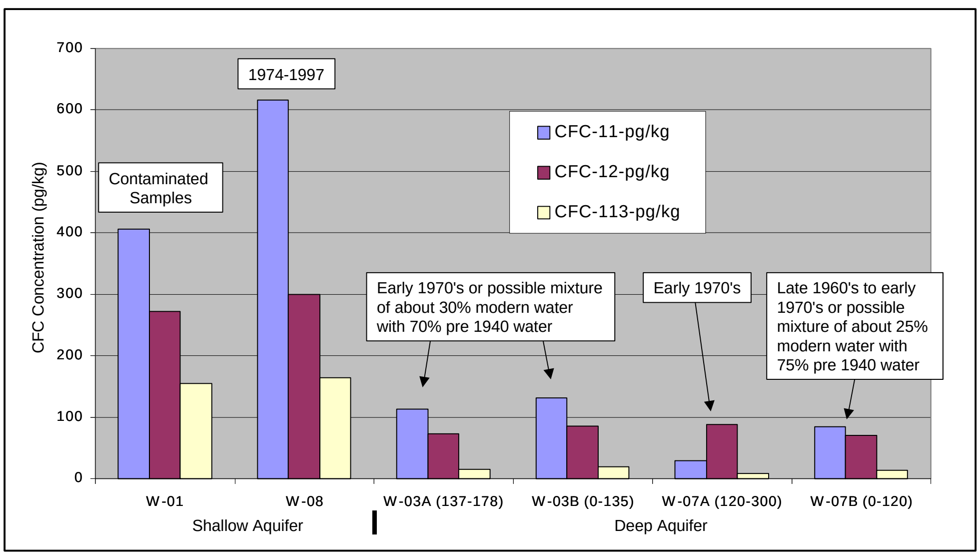

Figure 2.11a Groundwater age-dating analysis results using CFC's. Wells completed in the deep aquifer had lower concentrations of CFC's than shallow aquifer indicating older waters.

The samples from the shallow aquifer were characterized by high levels of CFC's in both W-01 and W-08 and are considered to be contaminated by modern air (Nelms, personal commun., 2001). The samples from W-03 and W-07 had age dates from the late 1960's to early 1970's or a possible mixture of about 25-30% modern water with 70-75% pre-1940 water (fig 11a). Relatively high levels of NO_3^- are noted in the shallow aquifer in W-01 and W-08 but the deep aquifer sampled from W-03 and W-07 had only 7-20% of the NO_3^- detected in the shallow aquifer (fig. 2.11b). The shallow aquifer water samples had only 39-49% of the mean equivalent cations and anions found in the deep aquifer samples (fig.2.11c).

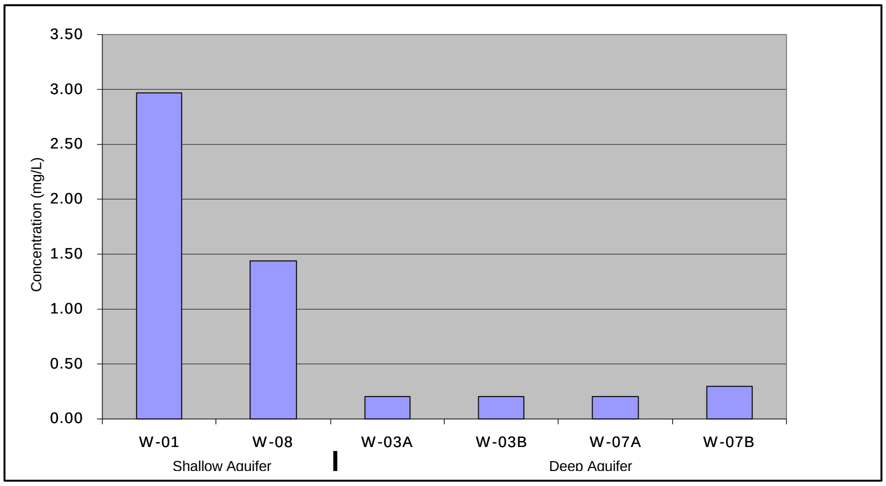

Figure 2.11b Results of water chemistry analysis. Higher concentrations of NO_3- in the shallow aquifer may be due to its proximity to fertilizers at the land surface.

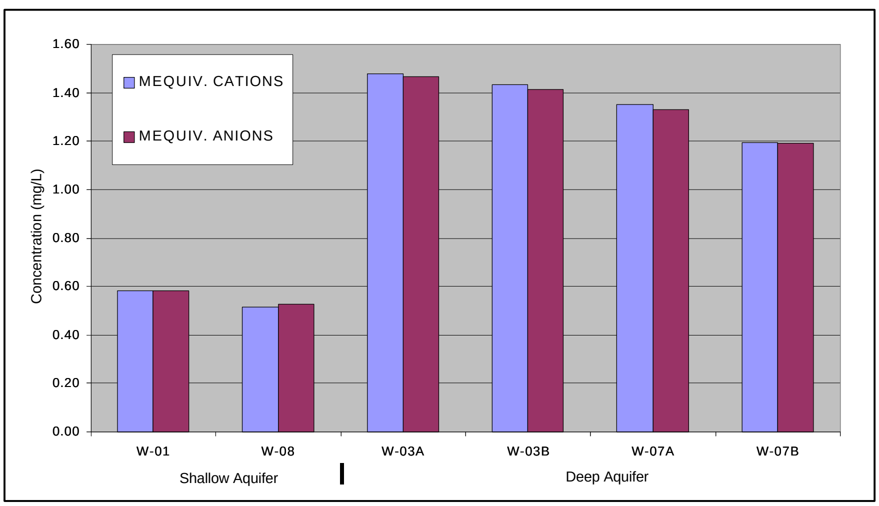

Figure 2.11c Mean equivalent cation and anion results. Exposure of groundwater to rock surfaces for typical residence time in the deep aquifer allows for continued dissolution of anions and cations.

The CFC analysis suggests that the shallow aquifer contains predominantly modern water. Personal communication with water well drillers indicates that the water quality in the shallow aquifer throughout the Blue Ridge Province can deteriorate due to increased turbidity soon after major rain events. The relatively high levels of NO_3^- in the shallow aquifers may originate from NO_3^- enriched fertilizers in use at the field site. These factors strongly imply rapid recharge of the shallow aquifer from precipitation and are primary reasons why the shallow aquifer is generally not considered by water resource authorities as a potable water source in new water wells. The relatively old CFC age dates for the deep aquifer indicate a long cycle time for these waters and that the fractured bedrock in the subsurface has been exposed to groundwater for significant periods of time allowing for dissolution and release of cation and anions into the groundwater. The higher levels of Ca^{2+}, Mg^{2+}, K^+, Fe^{2+}, and Mn^{2+} in the deep aquifer compared with the shallow aquifer support this.

A NEW CONCEPTUAL MODEL OF BLUE RIDGE AQUIFERS

Shallow Aquifer

Currently used aquifer models for the Blue Ridge Province use are based on a conceptualization that involves a shallow water table aquifer serving as the main storage reservoir in direct communication with underlying fractured bedrock (figure 2.1). In our experience the shallow aquifer has significant geologic variability and is often first encountered during drilling as a thin, confined aquifer at the base of the saprolite concomitant to the top of bedrock ("first water" in driller's terminology), or locally as a water table aquifer where the overlying unsaturated zone is permeable to water from precipitation (Seaton and Burbey, 2000).

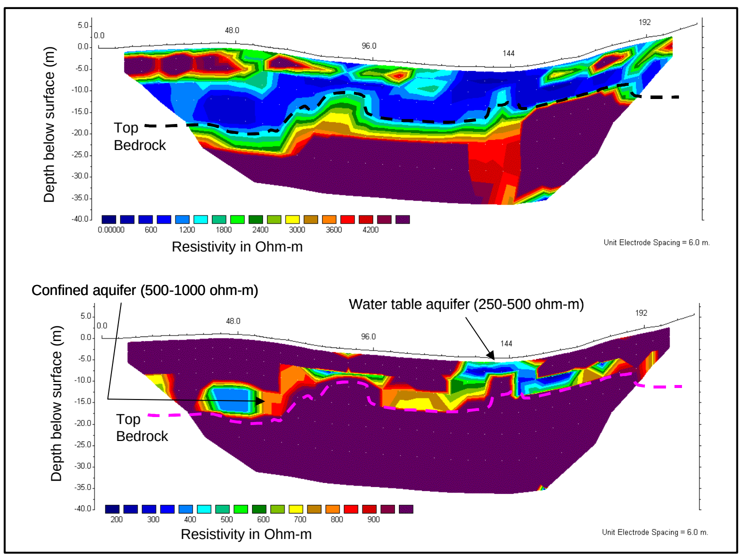

Figure 2.12 Resistivity profile 8 showing significant variation in resistivities in shallow aquifer. Top profile has color scale set to resistivity range of entire profile. Color scale on bottom profile limited to resistivity range of shallow aquifer.

Geologic variability in the shallow aquifer at the research site is illustrated as significant contrasts in subsurface resistivity in the resistivity profile presented in figure 2.12. Water table conditions in permeable saprolite are 250-500 ohm-m zones in the shallow subsurface. Other areas associated with confined aquifer conditions in the shallow aquifer produce resistivities from 500 to over 1000 ohm-m. Confined conditions were observed following drilling operations in 6 of the wells at the research site as water levels stabilized several feet above the top of the shallow aquifer. Confined conditions as described here have been reported to occur throughout the Blue Ridge and Piedmont provinces. (personal communication with water well drillers and field personnel, 1996-2001). Daniel (1996) and Daniel and Harned (1997) noted that a relatively low permeability zone in the upper regolith often overlies a higher permeability transition zone of concentrated water flow at the base of the saturated saprolite adjacent to the top of bedrock in the Piedmont Province of North Carolina. Stewart, et al. (1964) and Nutter and Otton (1969) reported similar conditions in the regolith in the Piedmont province in Georgia and Maryland respectively.

The drilling of well W-10 caused the shallow and deep aquifers to become hydraulically connected via the wellbore and illustrates the natural hydraulic separation of these units. Figure 2.13 illustrates the well logs from W-10.

The shallow aquifer is hydraulically isolated from the deep aquifer by impermeable bedrock at the field site. Pairs of wells testing the static water levels in the shallow and deep

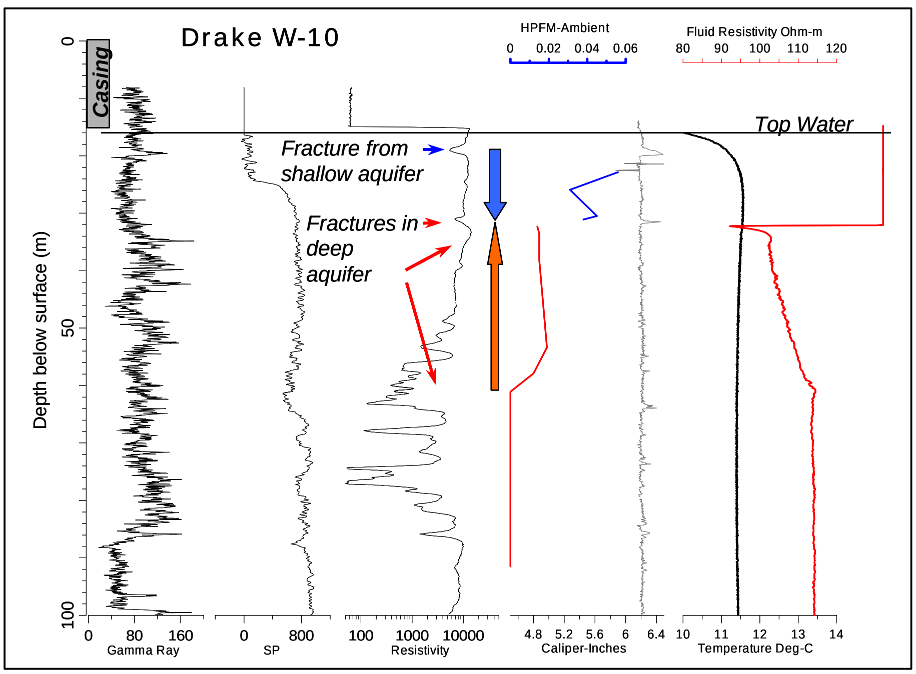

Figure 2.13 Borehole logs from Well W-10. Upflow from fracture in deep aquifer meets downflow from shallow aquifer in an open fracture above the fault plane surface.

aquifers document the greatest separation of head values in the northern part of the site (fig. 2.6c). Wells W-01 and W-02 are completed in the shallow and deep aquifers, respectively, and are separated horizontally by 12 m at the land surface. The average head values measured in the shallow aquifer in W-01 are 16.8 m above the measured heads in the deep aquifer in W-02. The average separation distance between the shallow and deep aquifer head values decreases to 2.2 m in well pair (W-07 – W-08) in the east central part of the site. The heads for the shallow aquifer are slightly lower than the deep aquifer heads in well pairs (W-03 – P-01) and (W-09 – W-06). The heat pulse flow meter (HPFM) results from this well indicate that down-flow occurs in the interval from 19 to 31 meters below the surface and up-flow occurs from 61 to 31 meters under ambient conditions. The down-flow occurs from the shallow aquifer into an open fracture in the bedrock. The up-flow occurs from the deep aquifer into the same open fracture located below the static water level of both the shallow and deep aquifers. These opposing flows indicate the head differences and the presence of an aquitard between these two aquifers. Daniel (1996) and Daniel and Harned (1997) noted that a poor connection may exist between the shallow aquifer and the deep bedrock fractures in the Piedmont of North Carolina.

Aquifer testing also reveals very low vertical hydraulic conductivity between the shallow aquifer and the deep underlying bedrock fractures. Aquifer tests conducted in the fractured bedrock caused minimal drawdown in nearby wells in the overlying shallow aquifer. Aquifer testing of the bedrock aquifer over a 6-day period produced approximately 24 meters of drawdown in the fractured aquifer (figure 2.8a) but only a maximum of 0.16 meters of drawdown in the overlying shallow aquifer (figure 2.8b). The drawdown in the shallow aquifer is the greatest in an area in the southern end of the site suggesting a zone of preferential communication between the shallow and deep aquifers. This communication may be accomplished by large masses of intensely fractured vein quartz that cut across the confining bedrock separating the shallow and deep aquifers. Outcrops of massive vein quartz are common in the Blue Ridge Province and present in the area where the greatest drawdown from the aquifer test occurred in the shallow aquifer.

These data and rock cuttings from drilling operations indicate that the base of the shallow aquifer is bounded by a very low permeability bedrock-confining unit that separates the shallow aquifer from the deeper fractured bedrock aquifer. This confining unit is locally breached which allows enhanced drawdown to occur in selected wells in the shallow aquifer when the deep fractures are pumped. Aquifer tests conducted in the shallow aquifer separately at the field site typically yield 1-11 l/m under confined conditions and 7.5-11 l/m when water table conditions prevail. The low yield and limited thickness of this aquifer diminish its role as a storage reservoir for the deep aquifer system. The shallow aquifer is likely recharged in areas where there is direct contact with surface waters or locally where water table conditions exist.

Deep Aquifer in Fractured bedrock

The deep fractured aquifer has significant geologic variability including fault shear zones as observed in the surface resistivity profiles, logged boreholes, and direct observations from outcrops (Seaton and Burbey, 2000). The fracture network may include highly transmissive fractures directly overlying the fault shear zones that are associated with brecciated granulite gneiss above the ancient thrust faults.

The ground surface and the contoured water-level surface from the deep aquifer converge at the bottom of the field site in the vicinity of a perennial spring (figs. 2.5, 2.6a-b). The primary source of recharge to the deep aquifer may be the area-limited zone where the ground surface and the potential surface from the deep aquifers meet. The water level of the shallow aquifer is also approximately at the same elevation as the topographic surface and deep aquifer in the southern part of the field site (figure 2.6c). Large masses of fractured vein quartz have been observed to outcrop in this area and also have been encountered during the drilling of well W-05. Vein quartz commonly occurs throughout the Blue Ridge and Piedmont provinces as a by-product of low-grade metamorphism. Under the elevated temperatures and pressures experienced in these provinces during times of tectonic stress and deep burial, quartz could mobilize and accumulate along fractures or fault planes. Subsequent cooling and fracturing of the massive quartz could provide paths for vertical movement of groundwater. This fractured quartz may breach the hydraulic barrier between the shallow and deep aquifers and also provide a pathway for recharge or discharge of the deep aquifer.

A schematic representation of the new conceptual model for Blue Ridge aquifers is shown in figure 2.14. Conceptually within this model the shallow aquifer is hydraulically separated from the deep fractured bedrock aquifer by a low permeability confining unit. Recharge to the deep aquifer may occur via slow downward flow from the shallow aquifer or through localized breaches in the confining unit that separates the shallow and deep aquifers. Recharge to the shallow aquifer can occur in areas where unconfined conditions exist or where surface waters are in direct communication with the shallow aquifer. Significant geologic complexity associated with ancient thrust faulting exists within the deep bedrock in the Blue Ridge Province. High transmissivity zones parallel and overlying the thrust plane surfaces may be the major conduits for fracture flow in this system. A secondary interconnected set of fractures with lower hydraulic conductivity also exists in the bedrock. Together this fracture network provides the storage “container” and the pathway for groundwater movement. Limited areal extent of fracture networks reduces the storage volume of these aquifers and tends to compartmentalize the deep aquifer systems.

CONCLUSIONS

Groundwater flow in the Blue Ridge Province is a relatively complex process that is controlled by the geologic variability in the subsurface. The flow system is usually composed of a shallow aquifer located in the unconsolidated saprolite and shallow portions of the bedrock overlying a deep fractured bedrock aquifer. The shallow aquifer may be a relatively thin confined porous layer on the top of bedrock overlain by relatively impermeable silts and clays or it may be relatively thick, porous, and sand prone with a water table aquifer. The shallow aquifer has modern age waters, is rapidly recharged by precipitation, and prone to contamination by activities at the ground surface such as crop fertilization. The shallow aquifer is generally separated from the deep fractured bedrock aquifer by relatively impermeable bedrock causing substantial hydraulic head differences between these units under static and pumping conditions. Localized breaches in the confining bedrock layer may cause communication between the shallow and deep aquifers.

The bedrock fractures forming the deep aquifer may be caused by ancient thrust faults and also recent tectonism. Thrust faulting formed relatively horizontal planes of fractured rock that can have relatively high transmissivity and storage capacity. Other somewhat lower permeability fractures can be present forming an interconnected fracture network with the fault plane fractures. Groundwater in the deep aquifer is older than the waters of the shallow aquifer and can contain the major anions and cations that have dissolved out of the bedrock.

The conceptual model presented in this research incorporates the parameters from the previous model presented by Heath (1984) and also includes observations from previous research throughout the Blue Ridge Province from Maryland to North Carolina (Daniel 1996, Daniel and Harned 1997, Stewart, et al. 1964 and Nutter and Otton 1969), and personal communication with water well drillers and water resources personnel currently working in the area (1996-2002).

Many of the existing regulations regarding wellhead protection, watershed management, and sewage-wastewater disposal in the Blue Ridge Provence are based on the older and relatively simple model of Blue Ridge aquifers. This new conceptual model underscores the need to locate and protect the localized watersheds and recharge areas responsible for supplying water to the aquifers. Current regulations require that wells be drilled at certain minimum distances from surface features or sources of contamination. These regulations may have a limited effect on reducing contamination if the underlying geology is not more fully considered. Understanding the variability of the bedrock geology and the potential for high transmissivity bedrock fractures can also provide insights allowing more accurate location of high yielding water supply wells and a more realistic understanding of the volume of water available from these wells.

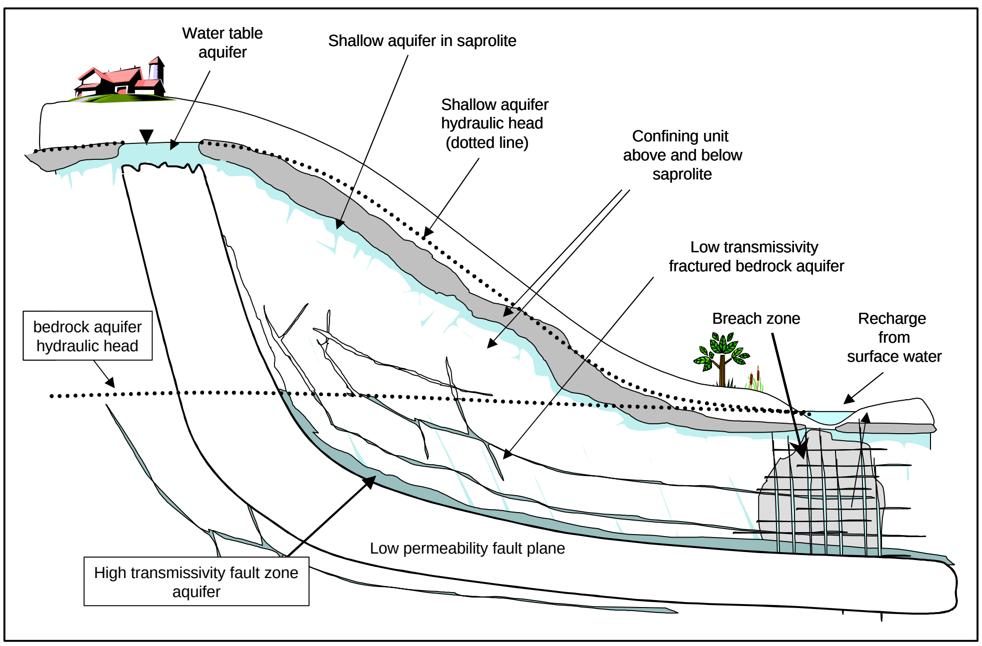

Figure 2.14 Conceptual model for groundwater flow in the Blue Ridge Province. Geological cross section through shallow and deep bedrock aquifers.

Chapter 3: Evaluation of two-dimensional resistivity methods in a fractured crystalline-rock terrane

ABSTRACT

A series of two-dimensional resistivity profiles collected in the Blue Ridge Province of southwest Virginia and results from numerical modeling of synthetic data reveal substantial differences in depth of investigation, resolution, and sensitivity using Wenner, Schlumberger, dipole-dipole, and pole-pole data collection techniques. Resistivity profiles were collected using short (2 m electrode spacing, 48 m profile length), intermediate (6 m electrode spacing, 144 m profile length), and long (10 m electrode spacing, 240 m profile length) arrays over shallow unconsolidated soils and regolith overlying crystalline bedrock. Pole-pole data were only collected with the short array. Numerical modeling was used to simulate both vertical and horizontal structures similar to subsurface conditions in the field site.

All of the apparent resistivity data were inverted into earth models using a computer program that uses an l_1 norm smoothness constrained inversion technique. Earth models generated from both field data and numerical modeling acquired by the dipole-dipole technique consistently indicated more detail and greater depth of investigation than the other techniques. The dipole-dipole method uniquely imaged thin saturated sands and isolated high resistivity bodies beneath the 48 m length array, significant horizontal and vertical resistivity variation including a thick transitional resistivity zone in the 144 m length array, and anomalous low resistivity zones in crystalline bedrock in the 240 m length array. Earth models created from the Wenner and Schlumberger apparent resistivity data had a shallower depth of investigation and revealed significantly less geologic detail than the profiles generated from the dipole-dipole survey. The earth model from the pole-pole data had the greatest depth of investigation but low resolution and limited geologic detail when compared to the dipole-dipole survey.

INTRODUCTION

Two-dimensional resistivity profiling is commonly used for determining the distribution of electrical resistivity in the shallow subsurface. Subsurface resistivity data have been collected in environmental, geological, and archeological studies and can be correlated to degree of fluid saturation in the subsurface, lithology, porosity, and the ionic strength of subsurface fluids (Parasnis, 1997). Resistivity profiling gained renewed popularity during the 1990's with the introduction of computer-automated data collection systems and robust data inversion methods (Griffiths and Barker, 1993; Loke and Barker, 1996; Dahlin, 1996). Automated data collection allows hundreds of individual measurements to be made in a matter of hours while minimizing the manual labor previously needed for resistivity fieldwork. Commercially available inversion software for personal computers and advances in computer hardware have allowed for rapid processing and inversion of apparent resistivity field data for creation of two-dimensional resistivity earth models of the subsurface.

Several data collection schemes are available for subsurface resistivity studies. Each of these techniques take a series of voltage and current measurements from an array of electrodes placed on the ground surface along a line of profile. Commonly used data-collection techniques include: Wenner, Schlumberger, dipole-dipole, and pole-pole (fig. 3.1) among others.

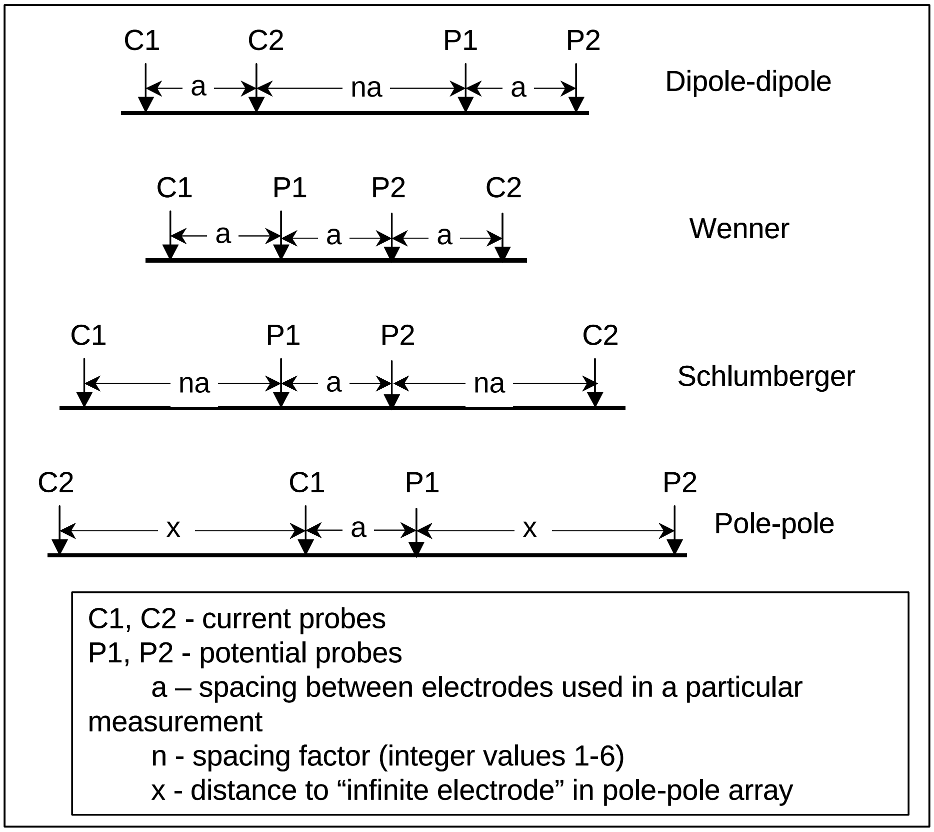

Figure 3.1 Conventional four-electrode arrays used for resistivity profiling in this study.

Each of these techniques has particular resolution, sensitivity, and depth penetrating capabilities. The previous research comparing array types was often based on one-dimensional soundings or profiles, possibly limiting their applicability when considering the problem of inverting two-dimensional apparent resistivity data. Dahlin and Loke (1998) have shown that one-dimensional modeling of apparent resistivity data give misleading results in relatively complex subsurface environments.

Most authors agree that the Wenner array has the best signal response and high resolution of horizontal structures but a relatively shallow depth of investigation and somewhat limited ability to detect vertical structures (Ward, 1990; Sharma, 1997; Reynolds, 1997; Loke, 1999). The Schlumberger method is considered to have good signal response, the ability to resolve horizontal and vertical structures relatively well, and greater depth of investigation than the Wenner array (Ward, 1990; Sharma, 1997; Reynolds, 1997; Loke, 1999). The dipole-dipole method has greater depth penetration than the Wenner and Schlumberger methods (Loke, 1999, Reynolds, 1997) but the lowest signal response of all the arrays (Ward, 1990; Sharma, 1997; Reynolds, 1997; Loke, 1999). Loke (1999) states that the dipole-dipole array is relatively good in resolving vertical structures but is poor in resolving horizontal structures. Ward (1990), Sharma (1997), and Reynolds (1997) have reported that the dipole-dipole array resolves horizontal structures fairly well, but is poor at resolving vertical features. The pole-pole method has the deepest penetration of all arrays and the widest horizontal coverage for a given array length but the poorest resolution (Loke, 1999, Robain, et al., 1999). The pole-pole method is also subject to telluric noise because of the long distance between the potential electrodes (Loke, 1999). The pole-pole method is commonly used in shallow archaeological studies and three-dimensional resistivity surveys requiring short spacing between electrodes.

This research uses apparent resistivity data from two sources: 1) the output of numeric modeling of synthetic geologic structures using a forward modeling program Res2Dmod (Loke, 2001) and 2) field data collected in the field site in the Blue Ridge mountains of southwest Virginia. A primary goal was to determine which array produced the highest quality data for input into an inversion routine to produce two-dimensional earth models. Evaluation of these resistivity data-collection techniques was made as part of a hydrogeologic investigation within the crystalline bedrock aquifers of the Blue Ridge Province in Virginia (Seaton and Burbey, 2000). The main objectives of using resistivity profiles in this environment are 1) to resolve the stratigraphic variability and water saturation in the shallow unconsolidated aquifers, 2) ascertain the lithologic variation in the crystalline bedrock, and 3) determine the location and shape of any structural features that may be controlling the movement of groundwater. The subsurface geology in the area of interest contains discrete resistivity zones in a wide variety of orientations. Other goals of this research include maximizing the depth of investigation and sensitivity to geologic detail while minimizing data acquisition time and simplifying field logistics. The primary resistivity data collection methods considered in this research include: Schlumberger, Wenner, and dipole-dipole techniques. In addition, the pole-pole method was used on a single profile and compared to the other methods for this line.

FIELD SITE

The field site resides on a farm situated in mountainous terrain 30 kilometers southwest of Roanoke, Virginia in the Blue Ridge Province in Floyd County, Virginia (fig. 1.1). The subsurface consists of a shallow layer of unconsolidated soil and weathered rock varying in thickness from 0 to 20 meters underlain by crystalline bedrock that is composed of metamorphosed igneous and sedimentary rocks including granite gneiss, biotite gneiss, mica schist, phyllite, and massive vein quartz. The bedrock is variably fractured and faulted making for a highly heterogeneous hydrogeologic system. The area averages 30-40 inches (75-100 cm) of precipitation annually with infiltration rates and saturation content highly dependent upon the subsurface geology.

METHODS FOR INVESTIGATION

Apparent resistivity data used in this study consists of synthetic data generated from numerical models and field data collected at the field site. Resistivity field data were collected with a Campus Geopulse earth resistivity meter and a 25-electrode cable with 10 meters between each electrode take-out. The selection of electrode combinations used for current and potential probes for each type of survey was based on Loke (1999) with the intent of providing high resolution resistivity data and maximizing the depth of investigation while minimizing noise and overly redundant measurements. At least two resistivity measurements were taken at each measurement point and then compared with each other. A resistivity value that was within 3% of the previous measurement at the point was accepted as a valid datum measurement.

Measurements with greater than 3 percent error were rerun with higher current, if possible, to lower the percent difference between compared values. Recorded data resulting from anomalous measurements were removed prior to the creation of the final inverse models. When acceptable measurements were collected at each measurement point in the survey, the composite set of values constituted the apparent resistivity data set.

The Res2dinv resistivity inversion software (Loke, 1999) was used to automatically invert the apparent resistivity data from the field and forward modeling into two-dimensional resistivity earth models. This software has two different inversion routines for creation of earth models from resistivity field data. The default inversion routine used by this program is based on an l_2 norm the smoothness-constrained least-squares method (deGroot-Hedlin and Constable 1990; Sasaki 1992). This inversion method minimizes the square of the differences (L_2 norm) between the measured and calculated apparent resistivity values and produces earth resistivity models with gradual transitions across zones of different resistivities. The second inversion routine within Res2dinv is called "robust inversion" which is an l_1 norm regularized inversion method (Ellis, et al. 1993). This method minimizes the absolute difference between the measured and calculated apparent resistivity values (Claerbout and Muir, 1973). Inversion with l_1 norm usually produces earth resistivity models with relatively sharp boundaries between resistivity zones, but within resistivity zones the resistivity usually has limited variation (Loke, 2000).

Our experience indicates that the l_1 norm inversion technique is most suited to the geology in the Blue Ridge Province. The interface between the regolith and bedrock, high saturation variability in the unsaturated zone, the location of the top of the water table aquifer, and also lithologic transitions within the bedrock, tend to represent sharp resistivity boundaries.

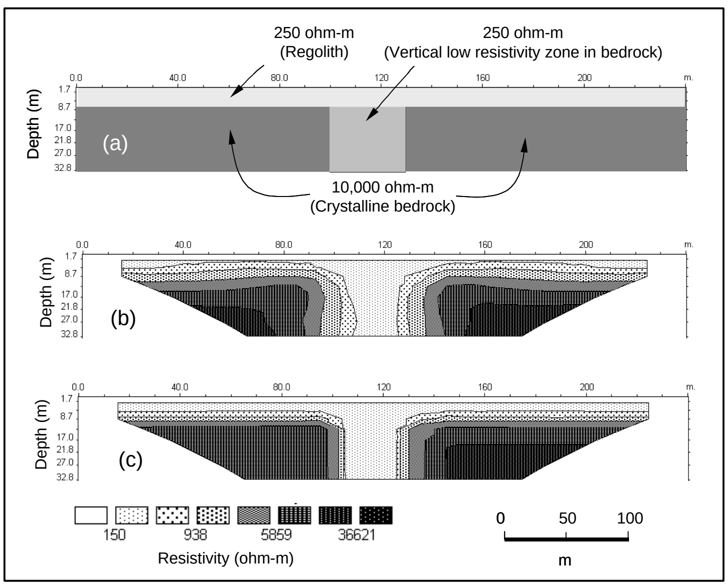

Figure 3.2 Comparison of earth resistivity models generated from the two different inversion techniques applied to the same synthetic apparent resistivity data set (dipole-dipole array). Starting resistivity Earth model (a), resistivity Earth model from L_1 norm inversion (b), resistivity Earth model from L_2 norm inversion (c).

Figure 3.2 is a comparison of earth resistivity models generated from the two different inversion techniques applied to the same synthetic apparent resistivity data set. The synthetic data were based on resistivities observed in the Blue Ridge province for the unconsolidated layer (250 Ω-m), crystalline bedrock (10,000 Ω-m), and an anomalous low resistivity zone within the bedrock (250 Ω-m). The least-squares inversion produced an earth model with broad and curved transitions between the different resistivity zones. The resistivity earth model resulting from the robust inversion has more linear and relatively sharper resistivity zone boundaries and appears to be the most similar to the starting model. Comparison of the l_1 norm and l_2 norm inversion methods with a real data case (northern portion of profile 4) in figure 3.3 shows similar results as the synthetic data tests. The earth model from the l_2 norm inversion shows gradual resistivity transitions between the high resistivity zones (6400 Ω-m) in the left-center part of the model to the lower resistivity zone (400 Ω-m) in the center. The l_1 norm inversion produced an earth model with relatively homogeneous high and low resistivity zones and thinner transitions between different zones.

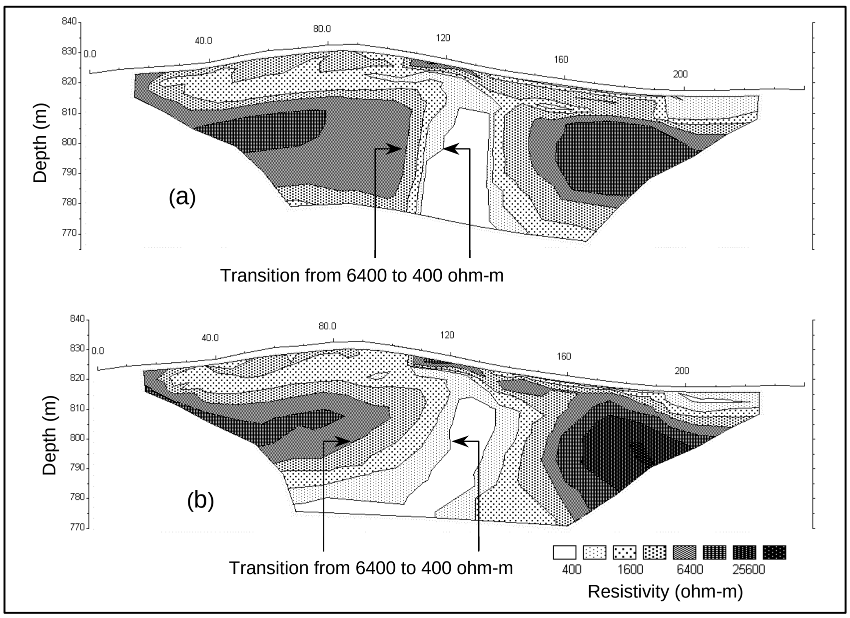

Figure 3.3 Comparison of the l_1 norm (a) and l_2 norm (b) inversion methods with a real data case (Line T-1 collected with dipole-dipole array).

NUMERICAL MODELING

Numerical modeling was accomplished using two synthetic resistivity models containing horizontal and vertical structures with varying resistivities (figs. 3.4a-b) as the input to the forward modeling code Res2Dmod (Loke, 2001). Forward modeling was accomplished by using Wenner, Schlumberger, dipole-dipole, and pole-pole techniques on a simulated 25-electrode (48 m length) array with 2m spacing between electrodes. The resulting apparent resistivities from the forward modeling were input into Res2Dinv (Loke, 2000) and inverted into earth resistivity models that are overlain on the starting synthetic models (figs. 3.5a-b).

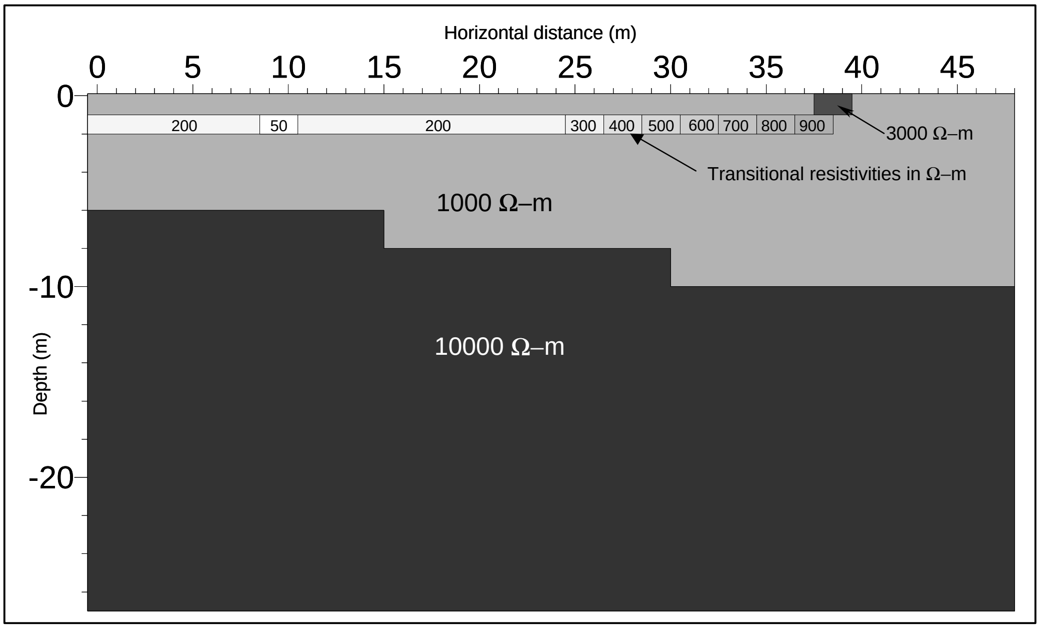

Figures 3.4a Starting synthetic horizontal model for the numerical forward modeling using Res2Dmod.

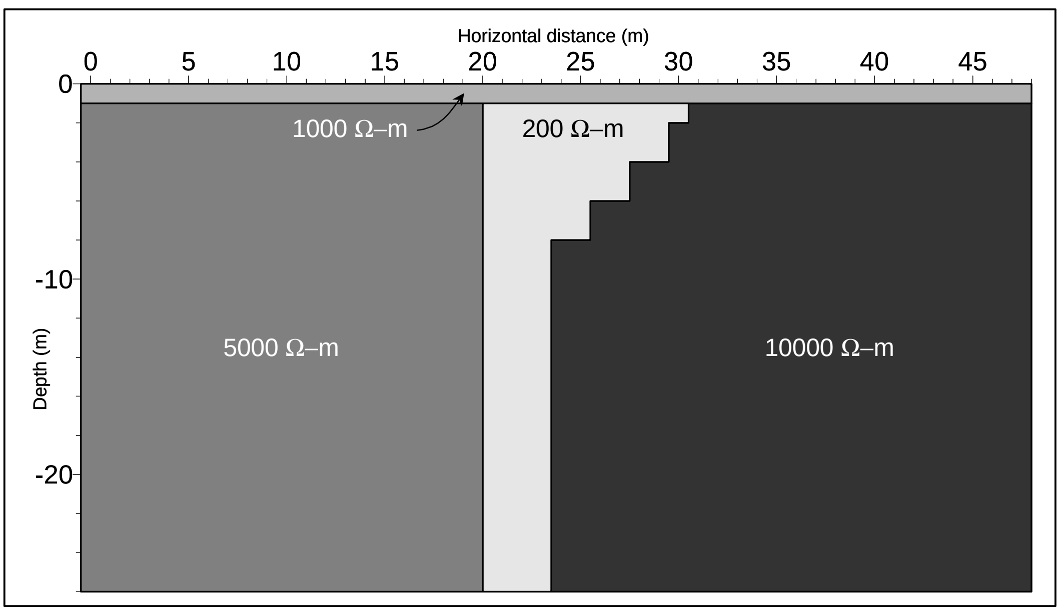

Figures 3.4b Starting synthetic vertical model for the numerical forward modeling using Res2Dmod.

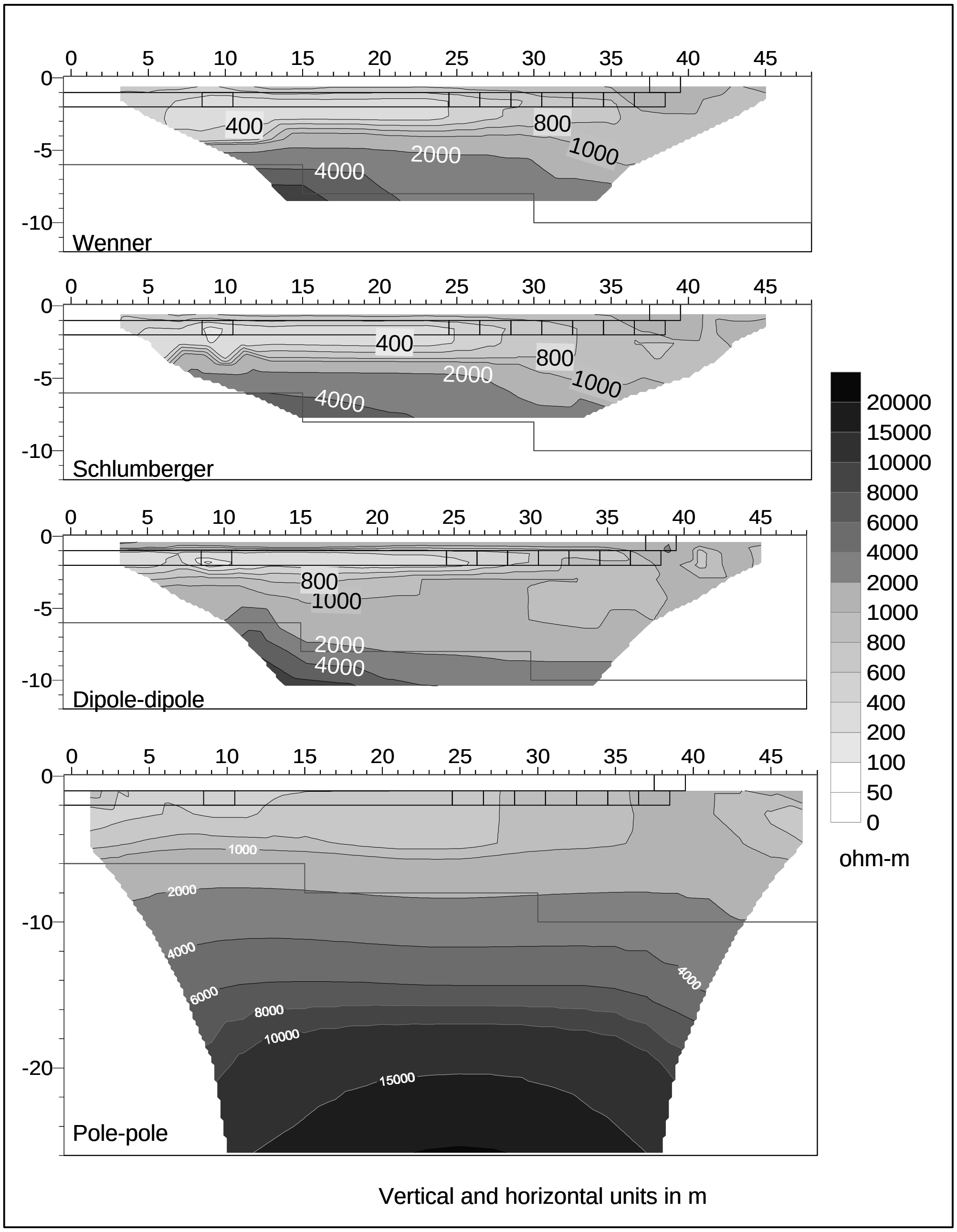

Figure 3.5a Resulting inverted earth models for each data collection method. Inverted earth models are overlain by the starting synthetic horizontal earth model.

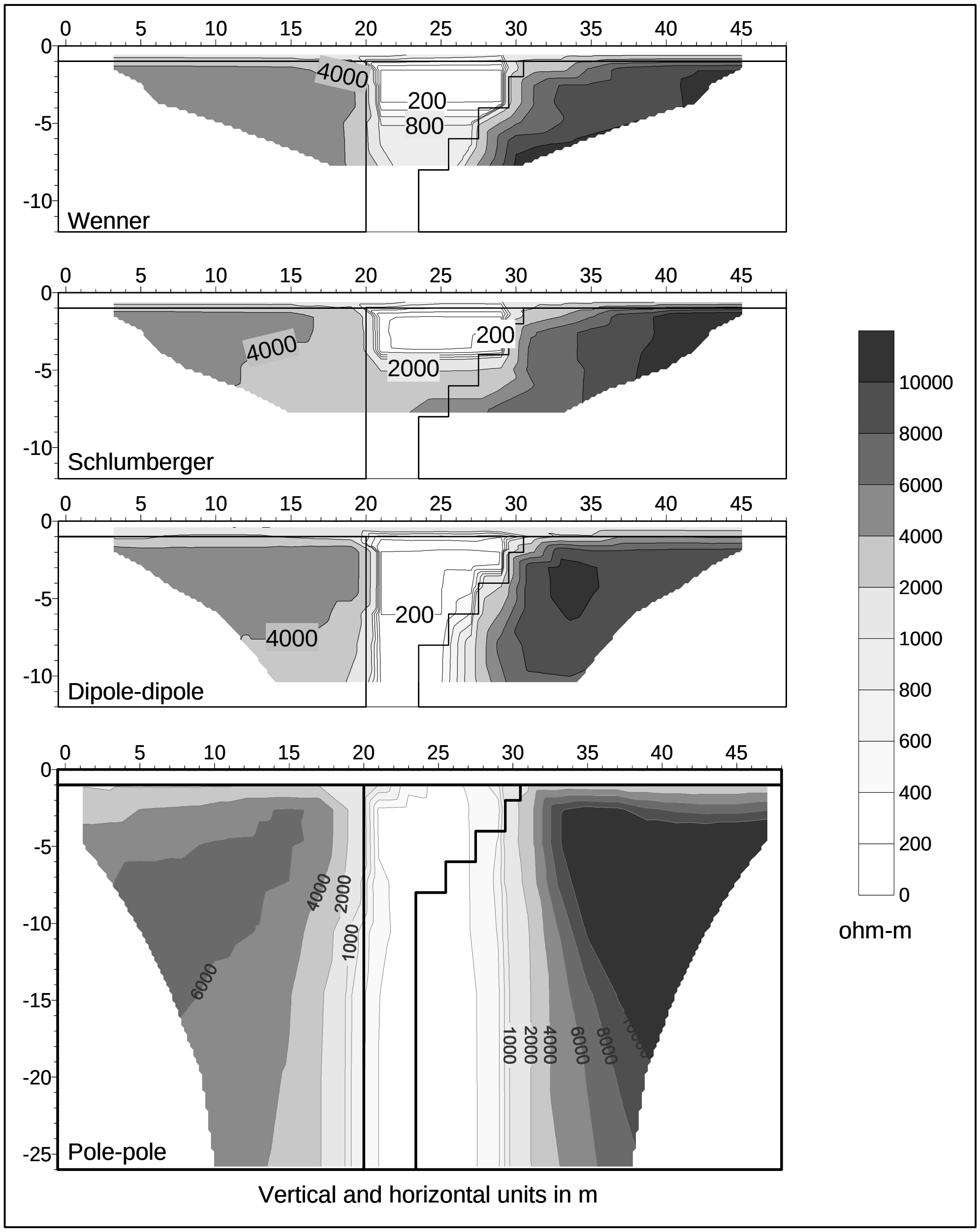

Figure 3.5b Resulting inverted earth models for each data collection method. Inverted earth models are overlain by the starting synthetic vertical earth model.

The horizontal model contains a 1 m thick shallow horizontal layer 1 to 2 m in depth that extends from the left edge of the model 38.5 m to the right. The right side of this layer has transitional resistivities varying from 200-900 Ω-m. The left side of the layer is set at 200 Ω-m except for an anomalous zone of 50 Ω-m located from 8.5 to 10.5 m horizontally. A small 3000 Ω-m zone is placed between 37.5 and 39.5 m horizontally and extends from the surface to a depth of 1 m. A 1000 Ω-m layer surrounds the shallow horizontal layer and extends downward to a sloping interface between 6 and 10 m in depth. Below this interface is a 10000 Ω-m layer that extends to 27 m depth.

The vertical model has a 1 m thick 1000 Ω-m horizontal surface layer with three resistivity zones in the subsurface. A 200 Ω-m vertical zone is in the center of the model with a 5000 Ω-m zone on the left side of the model and a 20000 Ω-m zone on the right. The 200 Ω-m vertical zone in the center of the model decreases in width from 11.5 to 3.5 m in a stepwise manner from 0.5 m to 8 m in depth. Below 8 m depth the vertical zone is a constant 3.5 m in width.

FIELD INVESTIGATIONS

Apparent resistivity data were collected in the field using Wenner, Schlumberger, and dipole-dipole methods on linear electrode arrays with electrodes spaced at 2, 6, and 10 meters. The pole-pole method was utilized only on a single test with the 2 m electrode spacing array. Resistivities for the pole-pole survey were calculated using the exact geometric factor (Loke, 2000) and the distance to the “infinite electrodes” was 5 times the maximum C1-P1 distance. The locations for the 3 electrode arrays in this investigation are illustrated in Figure 3.6.

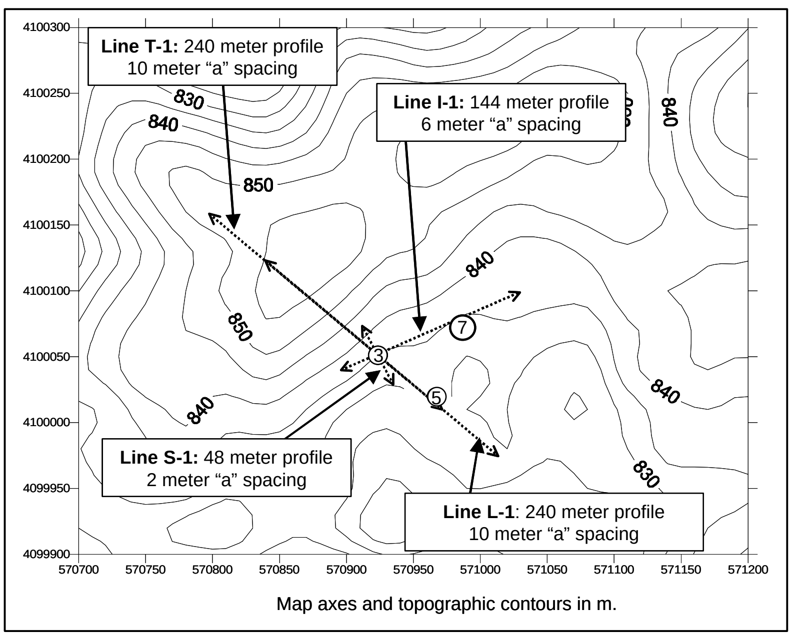

Figure 3.6 Locations for the 3 electrode arrays at the field site in southwest Virginia.

Each electrode array incorporated 25 electrodes using one of three different electrode spacings. Profile 9 was obtained using 2 m spacing (48 m length) and was located over a 10 m thick sequence of nearly horizontal sand and clay layers that directly overly bedrock. Resistivity measurements were collected with this array using Wenner, Schlumberger, and dipole-dipole methods during relatively high water table conditions (top of water table 1.83 m below surface) and then repeated approximately 24 months later during low water table conditions resulting from a prolonged dry spell (top of water table 3.11 m below surface). In addition, data were collected using the pole-pole method with the 2 m array during the low-water table conditions.

Profile I-1 was obtained using 6 m electrode spacing and is 144 m in length. Profile L-1 was obtained using 10 m spacing and is 240 m in length. Single sets of resistivity data were collected using Wenner, Schlumberger, and dipole-dipole methods for both profiles I-1 and L-1. These profiles were located over areas with variably thick regolith and heterogeneous bedrock.

The selection of electrode combinations used for current and potential probes for each survey was based on Loke (1999) with the intent of providing resistivity profiles with the highest resolution and maximum depth of investigation while minimizing noise and unnecessary measurements. The Wenner surveys were performed using all possible values of "a" for the given array. The Schlumberger and dipole-dipole surveys were performed with increasing values for "n" and "a" which attempts to provide a higher resolution earth model and maximize the depth of investigation (see Appendix A). Inversion parameters used in these tests are noted in Appendix B.

RESULTS AND DISCUSSION

Numerical Modeling

The inversion modeling of the synthetic data sets generally reflect the features seen in the starting models. With the horizontal model, each technique provided an inverted model showing transitional resistivities corresponding to the shallow transitional zone as well as increasing resistivities with depth that reflect the presence of the sloping high resistivity layer between 8 and 10 m depth. The Schlumberger and Wenner models overestimated the resistivities in the horizontal transitional layer by 100-200 Ω-m and showed this transitional layer to be twice as thick as the starting model. The Wenner model did not show the 50 Ω-m zone on the left side of the model and only a broad 2000 Ω-m zone in the vicinity of the 3000 Ω-m zone on the right side of the model. The 1000 Ω-m zone below the transitional layer is shown as a gradational interval. The deep 10000 ohm-m interval is at the very bottom of the Wenner and Schlumberger models and is expressed as a 4000-6000 Ω-m zone that is increasing in depth in a stepwise manner towards the right side of the model. The Schlumberger and Wenner models are very similar with the exception that the Schlumberger model has a lower resistivity response to the 50 Ω-m zone in the transitional layer. The dipole-dipole model shows a horizontal transition zone that is approximately the same thickness as the starting model but 100-200 Ω-m higher in resistivity. The dipole-dipole model shows a very small 100-200 Ω-m zone as the response to the 50 Ω-m zone in the transitional layer and a 1000-2000 Ω-m zone as the response to the small 3000 Ω-m zone on the right side of the starting model. The 1000 Ω-m zone below the transitional layer is shown as a broad relatively homogeneous interval with resistivities generally between 800-2000 Ω-m and the deep high-resistivity zone is shown as a 2000-6000 Ω-m zone sloping to the right. The pole-pole model shows the 1 m thick transitional layer as a 5 m thick zone with resistivities overestimated by 100-500 Ω-m. Layers of gradually increasing resistivity from 1000 to 15000 Ω-m represent the 1000 Ω-m zone and the deep 10000 Ω-m zone. The sloping interface between the 1000 Ω-m zone and the 10000 Ω-m zone is not evident in the pole-pole profile.

All of the tests using the vertical model showed the presence of the three deep-resistivity zones. The Wenner and Schlumberger methods produced rectangular 200 Ω-m resistivity zones in the shallow part of their profiles that increase in resistivity to 600-4000 Ω-m respectively with depth. These profiles have reproduced the right boundary of the low-resistivity zone as a sloping low-to-high resistivity interface. The Wenner profile has relatively homogeneous high resistivity zones on each side of the centrally located low resistivity zone while the Schlumberger profile has transitional yet high resistivity values in these areas. The dipole-dipole profile shows a relatively consistent vertical 400 Ω-m low-resistivity zone that continues to the bottom of the profile. This profile reproduces the sloping and vertical portions of the low resistivity zone but shows the homogeneous high resistivity zones with relatively broad transitional high-resistivity values. The pole-pole profile has a completely vertical low resistivity zone without any indication of the inclined right boundary. The entire 200 Ω-m interval is expressed as a 300-400 Ω-m vertical zone with broadly gradational boundaries into the adjacent high resistivity zones.

In conclusion, the dipole-dipole array configuration reproduced the synthetic horizontal and vertical structures more closely than the other array configurations.

Field Data

A total of 13 resistivity data profiles were collected in the field for this investigation using Schlumberger, Wenner, dipole-dipole, pole-pole techniques. The 13 resistivity profiles had a total of 1846 individual apparent resistivity measurements with only 22 measurements (1.2 percent) not being repeatable within 3 percent difference from the initial measurement.

Substantial differences exist in the earth models that were generated from the data acquired by each of the resistivity collection techniques over the same subsurface conditions. Earth models using the 2 m array are shown in fig. 3.7 for both high and low water table conditions. Figure 3.8 illustrates the corresponding percent change in resistivity resulting from the change in water table conditions for the Schlumberger, Wenner, dipole-dipole methods shown in figure 3.7. Earth models from the 6 m and 10 m arrays are shown in figures 3.9 and 3.10a respectively.

The profiles that were acquired during high water table conditions using the dipole-dipole technique and the 2 m array (left side of fig. 3.8) show a thin low-resistivity zone parallel to the ground surface overlying higher resistivity material. This zone corresponds to a thin saturated sandy interval adjacent to the top of the water table. The materials below this zone are composed of alternating layers of thin sand and clay. Auger refusal occurred where the regolith grades into weathered rock and corresponds to resistivities generally greater than 1000 Ω-m on the dipole-dipole profile. The top of bedrock is not pictured and occurs below the bottom of the profile. Small high resistivity zones exist at the top right of the high water dipole-dipole profile and at the left of the low water dipole-dipole profile. A larger high-resistivity zone is present left of borehole 3, between 817 and 820 depths on the high water dipole-dipole profile.

The Schlumberger and Wenner techniques produced earth resistivity models that have more homogeneous low and high-resistivity zones associated with the unconsolidated layer. In addition, these models do not have direct indicators of the water table surface or discrimination

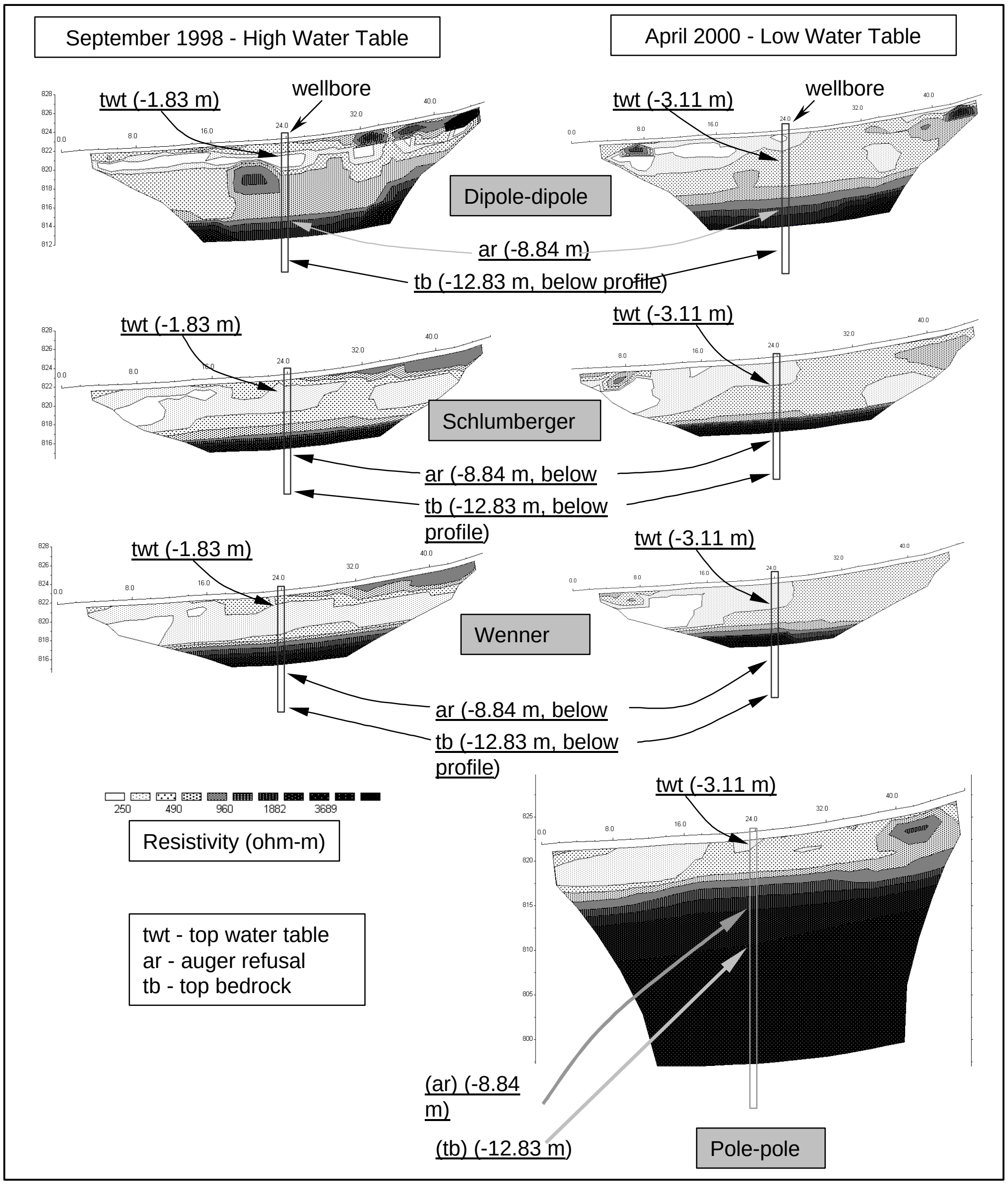

Figure 3.7 Comparison of earth models using the 2 m array. Top of water table (twt), depth of auger refusal (ar), and top of bedrock (tb) noted on each diagram.

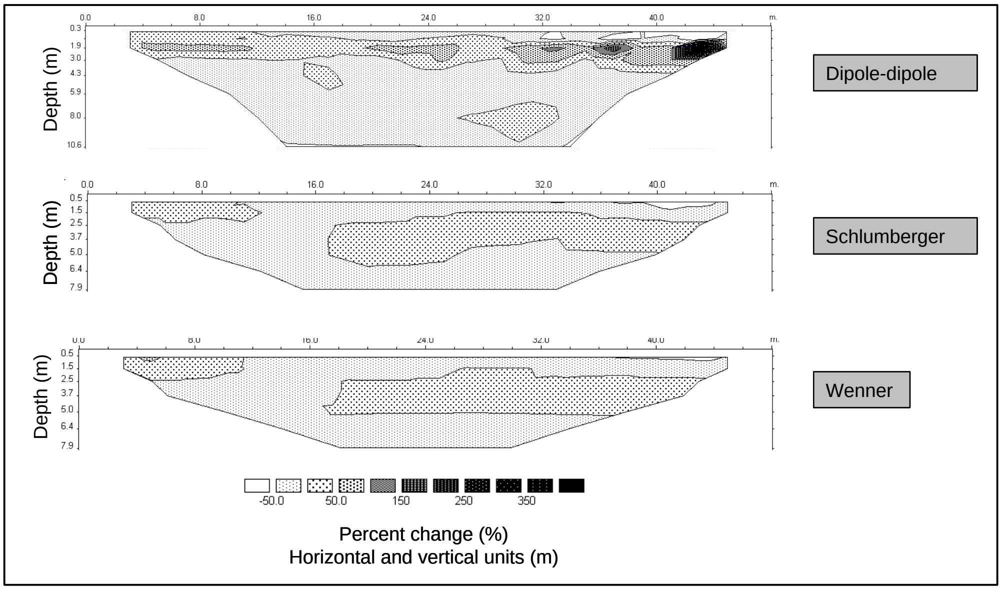

Figure 3.8 Comparison of percent change plots of 2m arrays in fig. 3.7

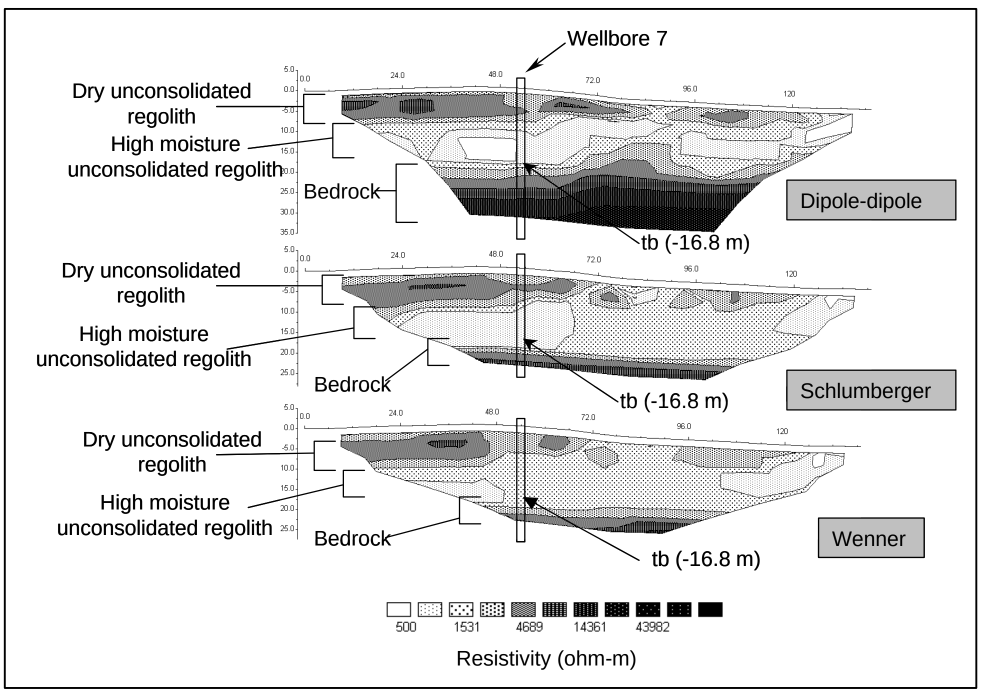

Figure 3.9 Earth models from the 6 m arrays.

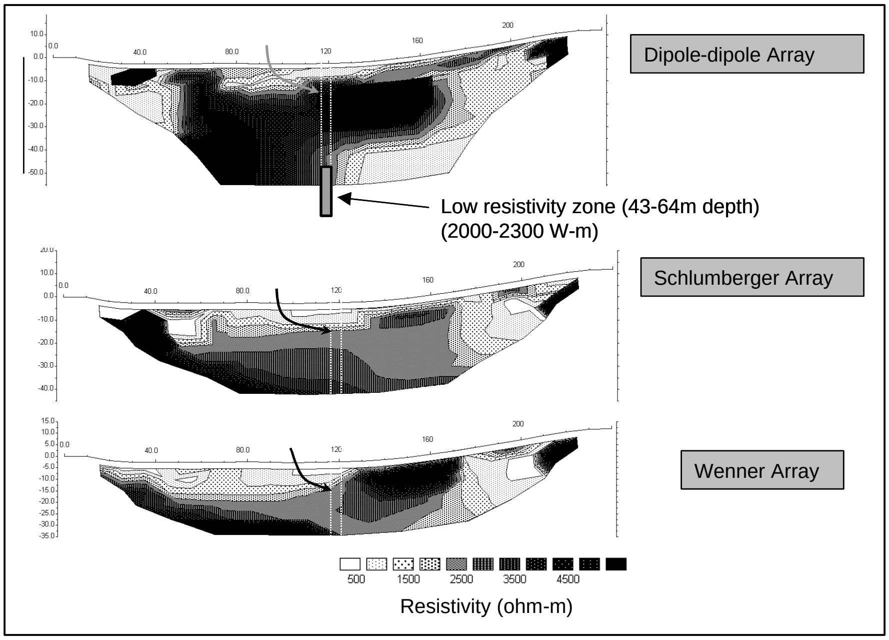

Figure 3.10a Earth models from the 10 m arrays.

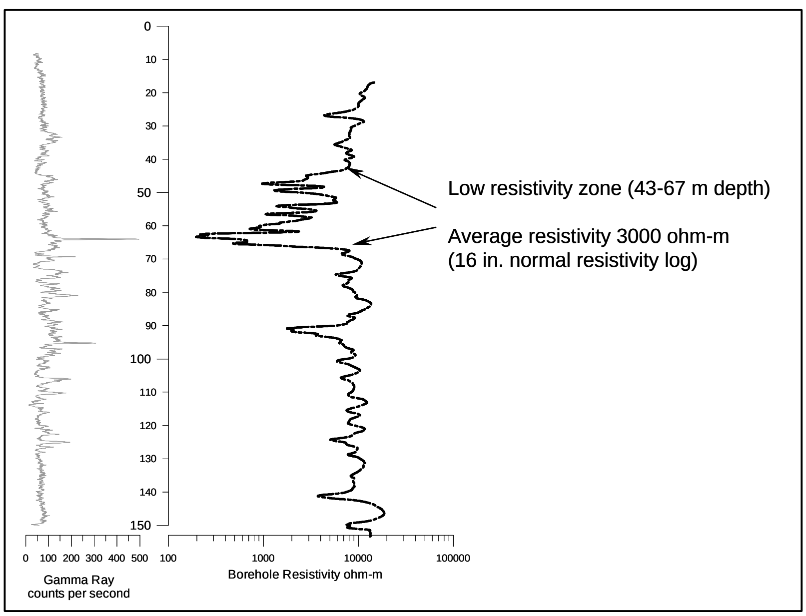

Figure 3. 10b 16-inch normal resistivity and gamma ray borehole logs from well 3.

of individual stratigraphic layers. The high resistivities displayed at the bottom of the profiles from the Schlumberger and Wenner data are typically associated with crystalline rock in this setting but occur anomalously here above the depth of auger refusal and above the top of bedrock. The data collected during low water table conditions (fig. 3.8 right side) resulted in profiles that generally show higher resistivities than high water table earth models. The thin low-resistivity zone near the surface of the dipole-dipole earth model profile has diminished in size with the lowering of the water table. The profiles generated using the Schlumberger and Wenner methods exhibit more homogeneous resistivity zones in the regolith than the profiles representing high water-table conditions. Figure 3.8 reveals that the greatest increase in resistivity (50-250%) from high to low water table conditions occurs along the thin sandy interval observed near the top of the profile generated by the dipole-dipole method. This change is attributed to dewatering of the sand due to the drop in water table elevation that corresponds to a lowering of the resistivity in this interval. The profiles generated from the Schlumberger and Wenner methods show that a general increase in resistivity (0-50%) occurs with the lowering of the water table.

The profile generated using the pole-pole method (fig. 3.7, bottom) reveals a homogeneous shallow lower resistivity (<1000 Ω-m) layer above a relatively homogenous high resistivity layer at an elevation of about 818 m. This profile has significantly greater depth of investigation than the others but less resolution and sensitivity within resistivity zones.

Earth models developed from the 6 m array resistivity data (figure 3.9) indicate 3 horizontal layers of resistivities with gradational resistivity zones between each layer. Borehole data adjacent to the line representing the 6 m array confirm the relationship of the different resistivity zones to the varying lithologies. The high-resistivity zone observed at the top of the profiles adjacent to the land surface is associated with dry semi-consolidated or unconsolidated regolith. The lower resistivity zone below this interval is caused by an increase in moisture content within the unsaturated zone. The deep higher resistivity horizontal layer is associated with crystalline bedrock. Borehole data indicate that the shallowest water zone on this profile is a 1 m thick confined aquifer directly overlying the bedrock.

The profiles generated by the dipole-dipole method extend to depths of 30-35 m, show significant variations in resistivity both vertically and horizontally, and have a thick transitional resistivity zone between the regolith and bedrock intervals. The Schlumberger and Wenner profiles reveal more discreet and homogeneous high and low resistivity zones, thinner transitional resistivity zones, and extend to depths of only 25-30 m.

The profiles generated from the 10 m array (fig. 3.10a) varied from 35 to 50 m in depth and reveal significant horizontal and vertical changes in resistivity. Borehole cuttings and geophysical well logs (fig. 3.10b) were used to correlate the different resistivity zones in the resistivity profiles to specific rock types. The profile generated from the dipole-dipole method has a large centrally located high-resistivity interval, indicative of crystalline bedrock, nearly surrounded by transitional and low-resistivity zones. The thin transitional resistivity zones located around the centrally located high-resistivity interval imply sharp geologic contacts around this interval. The lower resistivity zone above the bedrock interval represents unconsolidated regolith. The vertically aligned lower resistivity zone at the left end of the profile represents saturated, fractured vein quartz. The vertical low-resistivity zone at the right end of the 10 m profile and the horizontal lower resistivity zone at the bottom of the profile represent phyllitic rocks associated with fault plane surfaces within the bedrock. The profiles from the Schlumberger and Wenner methods do not show the deep horizontal lower resistivity zone or the vertically aligned lower resistivity zone on the left side of the profile observed in the dipole-dipole profile. Both the Wenner and Schlumberger methods produced profiles with gradational increases in resistivity with increasing depth within the high resistivity bedrock interval.

A 40.6 cm (16 inch) normal resistivity log from borehole 3 is shown in fig. 3.11 along with the vertical traces of earth-modeled resistivity from each of the surface resistivity profiles collected with the 10 m array.

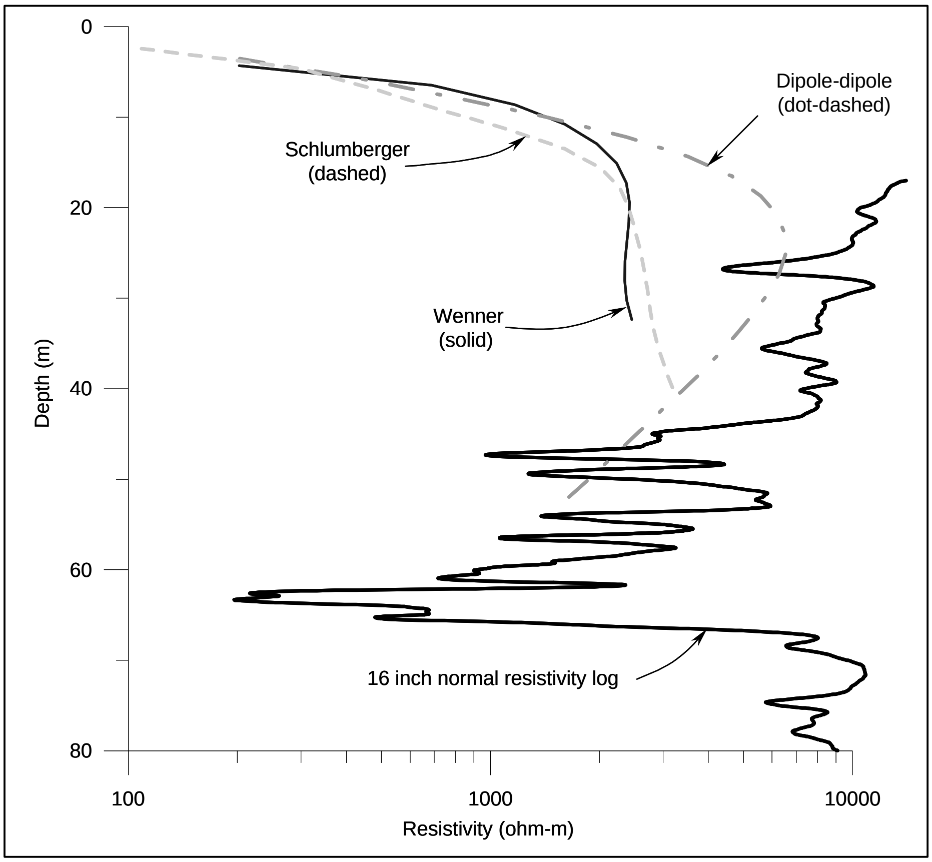

Figure 3.11 The 16-inch normal resistivity log from borehole 3 with the vertical traces of modeled resistivity from each of the surface resistivity profiles collected with the 10 m array.

The vertical traces of modeled resistivity from the surface resistivity profiles were taken from the location of borehole 3 on each the profiles. The modeled resistivity data from the dipole-dipole method approaches the logged resistivity data in absolute value and mimics the low resistivity zone (43-67 m) in the well log with a low resistivity interval starting at approximately 30 m. The model from the Schlumberger and Wenner methods underestimate the resistivities collected in the borehole and lack the depth of investigation to detect the low resistivity (43-67 m) interval in the borehole.

CONCLUSIONS

The orientation of potential and current electrodes that forms the basis of the different array types in surface-resistivity profiling has a substantial influence on the resolution, sensitivity, and depth of investigation of the surveys used in this investigation both in simulated numeric models and data acquired in the field. The arrays that have the potential electrodes placed inside the current path (Wenner and Schlumberger) have a shallower depth of investigation (fig. 3.12), generally less resolution and sensitivity to geologic detail than arrays with the potential probes outside of the current path (dipole-dipole). The pole-pole method used for the 2 m array had significantly greater depth of investigation than the other techniques but lower resolution and sensitivity than the other methods.

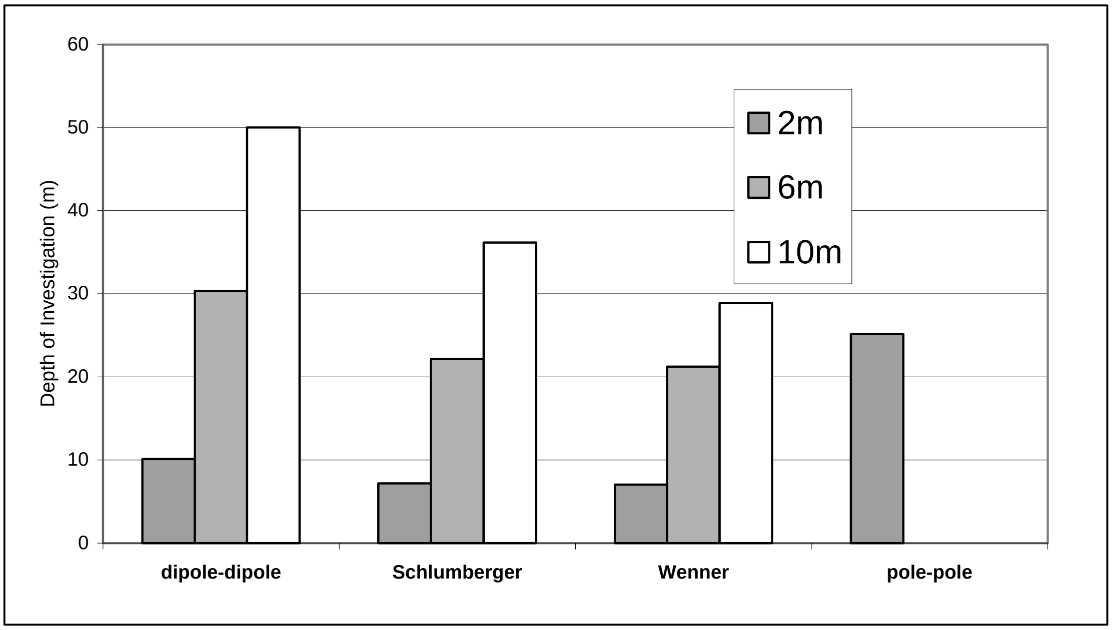

Figure 3.12 Comparison of depths-of-investigation for different array lengths and configurations.

The results of the numerical modeling indicate that the dipole-dipole method produces earth models most suited to meet the goals of our research. This technique reproduced the shallow horizontal transitional layer, the sloping high resistivity layer, and the intermediate depth 1000 Ω-m interval relatively accurately. The dipole-dipole method was also the most sensitive the small 50 and 3000 Ω-m intervals. In the vertical model the dipole-dipole technique reproduced the low resistivity vertical zone and its boundaries with the higher resistivity areas. In addition the dipole-dipole method has 20-25% greater depth penetration than the Wenner and Schlumberger methods. The Wenner method most accurately reproduced the high resistivity zones in the vertical model.

The pole-pole profiles had the greatest depth but showed the lowest resolution and least accurate rendering of the features in the starting models.

The results from the field data are in general agreement with the numerical modeling experiments. With the field acquired data, the Wenner and Schlumberger techniques produced similar smooth appearing earth model profiles but with a limited amount of the detail seen in the dipole-dipole profiles. The dipole-dipole profiles uniquely illustrated the shallow horizontal lower resistivity sand (high water conditions) from the 2 m array, the relatively broad transition zone between regolith and bedrock on the 6 m profiles, and the three low-resistivity zones surrounding the high-resistivity crystalline bedrock on the 10 m profiles. The Schlumberger and Wenner profiles for the 2 m and 6 m arrays have relatively homogeneous high- and low-resistivity zones associated with regolith and thin high-resistivity zones, usually associated with bedrock, that are located above the depths that these zones were encountered during drilling operations. For the 10 m array the Schlumberger and Wenner profiles contain broad transitional resistivities within the bedrock interval and only one low resistivity zones within bedrock. These arrays did not detect the deep horizontal lower resistivity zone found by the dipole-dipole survey and the normal resistivity well log.

The differences in the depth of investigation for these surveys is controlled by the “a” and “n” values used in the data collection. By increasing the “a” and “n” factors, the effective depth of investigation is increased. The dipole-dipole method has the greatest depth of investigation because of the ability to increase the spacing factor “n” between the C2-P1 electrodes to 6 (or more). Larger values of “n” can cause the signal strength to diminish rapidly below the background noise levels and the resolution of the resistivity meter. The Wenner method does not use a spacing factor thus limiting its overall effective depth of investigation when using a fixed electrode array. The Schlumberger method uses a spacing factor similar to the dipole-dipole method except that “n” is multiplied by the “a” spacing between both the C1-P1 and C2-P2 electrodes. This causes the overall length for each successive reading as “n” is increased to be longer than in the dipole-dipole method for the same “n” value. Ultimately the length of the cable limits the ability to use the Schlumberger method with large values of “a” and “n” together (Loke, 1999).

The dipole-dipole method was ultimately chosen to be most suitable for investigating the aquifers in the field site. The higher resolution, greater depth of investigation, and high sensitivity to geologic detail offered by the dipole-dipole method outweighed the fact that it used more measurements than the Wenner or Schlumberger methods. The Wenner or Schlumberger methods may be advantageous in areas where signal strength is diminished due to very conductive zones in the subsurface (Loke, 1999). The pole-pole method may be advantageous in situations requiring a depth of investigation that is below the limits of the dipole-dipole, Schlumberger, or Wenner techniques.

REFERENCES

Bartholomew, M.J., and Lewis, S.F., 1984, Evolution of Grenville massifs in the Blue Ridge geologic province, southern and central Appalachians, in M. J. Bartholomew, ed., The Grenville Event in the Appalachians and Related Topics: Geological Society of America, Special Paper 194, 229-254.

Bartholomew, M.J., Schultz, A.P., Lewis, S.E., McDowell, R.C., and Henika, W.S., 1999, Bedrock Geologic Map of the Radford 30 by 60 minute quadrangle, Virginia-West Virginia: Virginia Division of Mineral Resources, unpublished digital manuscript map

Brown, C.E., 1996, Vertical electrical resistivity and structural geometry of faulted, thermally altered and fractured clastic rock sequences and crystalline rock complexes of the north-central Culpeper Basin, Virginia: U. S. Geological Survey Open-File Report 96-0141, 24 p.

Choudhury, K., Saha, D.K., Rai, M.K., Naskar, D.C., and Ghatak, T.K., 1997, Geophysical surveys for hydrological and environmental studies in the eastern Calcutta metropolis: Indian Minerals, 51, no. 1&2, 41-56.

Claerbout, J.F. and Muir, F., 1973. Robust modeling with erratic data. Geophysics, 38: 826-844.

Costain, J.K., Hatcher, Jr., R.D., Coruh, C., Pratt, T.L., Taylor, S.R., Litehiser, J.J., and Zietz, I., 1989, Geophysical Characheristics of the Appalachian Crust, in Hatcher, R.D., Jr., Thomas, W.A., and Viele, G.W., eds., The Appalachian-Ouachita Orogen in the United States: Boulder, Colorado, Geological Society of America, The Geology of North America, v. F-2, p. 385-416

Dahlin, T., 1996, 2D resistivity surveying for environmental and engineering applications: First Break, v. **14.** no. 7, 275-284.

Dahlin, T. and Loke, M.H., 1998. Resolution of 2D Wenner resistivity imaging as assessed by numerical modeling. Journal of Applied Geophysics, 38: 237-249.

Daniel, C. C., 1989, Statistical analysis relating well yield to construction practices and siting of wells in the Piedmont and Blue Ridge provinces of North Carolina: U.S. Geological Survey Water Supply Paper 2341-A, 27 p.

Daniel, C.C., 1996, Ground-water recharge to the regolith-fractured crystalline rock aquifer system, Orange County, North Carolina: U.S. Geological Survey Water-Resources Investigations Report 96-4220, 59 p.

Daniel, C.C., III, and Harned, D.A., 1997, Ground-water recharge to and storage in the regolith-fractured crystalline rock aquifer system, Guilford County, North Carolina: U.S. Geological Survey Water-Resources Investigations Report 97-4140, 65 p.

Daniel, C.C., III, and Sharpless, N.B., 1983, Ground-water supply potential and procedures for well site selection, upper Cape Fear River basin (North Carolina): North Carolina Department of Natural Resources & Community Development, 73 p.

deGroot-Hedlin, C. and Constable, S., 1990. Occam's inversion to generate smooth, two-dimensional models form magnetotelluric data. Geophysics, 55: 1613-1624.

Donn, T.F., Baize, D.G., and Knight, B.T., 1989, Complications affecting ground water contaminant plume migration and delineation in the Piedmont: *In* Ground water in the Piedmont. Eds. C.C Daniel, III, R.K. White, P.A. Stone, Proceedings of a Conference on Ground water in the Piedmont of the Eastern United States, Clemson University, Clemson, S.C., 693 p.

Gernand, J.D., and Heidtmann, J.P., 1997, Detailed pumping test to characterize a fractured bedrock aquifer: Ground Water, 35, no. 4, 632-637.

Griffiths, D. H.; Barker, R. D., 1993, Two-dimensional resistivity imaging and modelling in areas of complex geology: Geophysical exploration in areas of complex geology: Proceedings 8th course of the International School of Applied Geophysics, Journal of Applied Geophysics, 29, n. 3-4, 211-226.

Gringarten, A.C., 1982, Flow-test evaluation of fractured reservoirs: Geol. Soc. of Amer. Special Paper 189, p. 237-263.

Haeni,F.P., Lane, J.W., Lieblich Jr., D.A.,1993, Use of surface-geophysical and borehole-radar methods to detect fractures in crystalline rocks, Mirror Lake area, Grafton County, New Hampshire: *In* Memoires of the XXIVth congress of the International Association of Hydrogeologists; hydrogeology of hard rocks Eds. D. Banks, S.B. Banks, 24, 577p.

Harned, D.A., and Daniel, C.C., III, 1992, The transition zone between bedrock and regolith: conduit for contamination?, In Ground water in the Piedmont. Eds. C.C Daniel, III, R.K. White, P.A. Stone, Proceedings of a Conference on Ground water in the Piedmont of the Eastern United States, Clemson University, Clemson, S.C., 693 p.

Heath, R.C., 1984, Ground-water regions of the United States: U.S. Geological Survey Water-Supply Paper 2242, 78p.

Henika, W,S., 1981, Geology of the Villamont and Montvale Quadrangles, Virginia: Virginia Division of Mineral Resources, Publication 35, 18 p.

Henika, W.S., 1992, Stratigraphy of the eastern Blue Ridge sequence in the Roanoke 30’x60’ quadrangle, Virginia: Geological Society of America, Abstract with Programs 24, no. 2, 21.

Henika, W.S., 2000, The Red Valley DDZ, A major basement detachment zone separating metasedimentary sequences of Eastern and Western Blue Ridge of S.W. Virginia, Geological Society of America Abstracts with Programs, vol.32, number 2

Isiorho, S.A. and Nkereuwem, T.O., 1996, Reconnaissance study of the relationship between lineaments and fractures in the southwest portion of the Lake Chad Basin; Journal of Environmental & Engineering Geophysics, 1, n. 1, 47-54.

Janardhana Raju, N., Reddy, T.V.K., and Nayudu, P.T., 1996, Electrical resistivity surveys for groundwater in the upper Gunjanaeru Catchment, Cuddapah District, Andhra Pradesh; Journal of the Geological Society of India, 47, 705-716.

Jenkins, D.N., and Prentice, J.K., 1982, Theory for aquifer test analysis in fractured rocks under linear (nonradial) flow conditions: Ground Water, v. 20, no. 1, p. 12-21.

Kruseman, G.P., and de Ridder, N.A., 1990, Analysis and evaluation of pumping test data. International Institute for Land Reclamation and Improvement, Pub. 47, Wageningen, The Netherlands, 377 p.

Lampshire, L.D., Coruh, C., and Costain, J.K., 1994, Crustal structures and the eastern extent of lower Paleozoic shelf strata within the central Appalachians: A seismic reflection interpretation, Geological Society of America Bulletin, v. 106, p. 1-18.

LeGrand, H.E., 1967, Ground water of the Piedmont and Blue Ridge provinces in the Southeastern States: U.S. Geological Survey Circular 538, 11p.

Loke, M.H. and Barker, R.D., 1996, Rapid least-squares inversion of apparent resistivity pseudosections using a quasi-Newton method: Geophysical Prospecting, 44, 131-152.

Loke, M.H., 1999, Electrical imaging surveys for environmental and engineering studies: A practical guide to 2D and 3D surveys: Pre-conference workshop notes W2, The theory and practice of electrical imaging, EEGS-European Section 5th Meeting, Budapest, Hungary.

Loke, M.H., 2000. Res2Dinv software version 3.44f.

Loke, M.H., 2001. Res2Dmod software version 3.00.

Nelms, D.L., and Harlow, Jr., G.E., 2001, Preliminary Results from Chloroflucarbon-Based Dating for Determination of Aquifer Susceptibility in Virginia: Virginia Water Research Symposium 2001, Charlottesville, Va.

Nutter, I.J., and Otton, E.G., 1969,Ground-water occurrence in the Maryland Piedmont: Maryland Geological Survey Report of Investigations no. 10, 56 p.

Paillet, F.L., 1995, Integrating surface geophysics, well logs and hydraulic test data in the characterization of heterogeneous aquifers: Journal of Environmental & Engineering Geophysics, 1, 1- 13.

Paillet, F.L., R.E. Crowder, and A.E. Hess, 1996, High-resolution flowmeter logging applications with the heat-pulse flowmeter: Journal of Environmental & Engineering Geophysics, 1, n. 1, 1-11.

Parasnis, D.S., 1997. Principles of Applied Geophysics, Fifth Edition, Chapman & Hall

Plummer, L.N., Busenberg, E., Bohlke, J.K., Carmody, R.W., Casile, G.C., Coplen, T.B., Doughten, M.W., Hannon, J.E., Kirkland, W., Michel, R.L., Nelms, D.L., Norton, B.C., Plummer, K.E., Qi, H., Revesz, K., Schlosser, P., Spitzer, S., Wayland, J.E., Widman, P.K., 2000, Chemical and isotopic composition of water from springs, wells, and streams in parts of Shenandoah National Park, Virginia, and vicinity, 1995–1999. U.S. Geol. Surv. Water Resour. Invest. Rept. 00-373, 70 pp.

Pratt, T.L., C. Çoruh, J.K. Costain, and L. Glover, III, 1988, A geophysical study of the Earth's crust in central Virginia; Implications for Appalachian crustal structure, Jour. of Geophys. Research, v. 93, p. 6649-6667

Reynolds, J.M., 1997. An Introduction to Applied and Environmental Geophysics. John Wiley & Sons, New York.

Robain, H., Albouy, Y., Dubas, M., Descloitres, M., Camerlynck, C., Mechler, P., Tabbagh, A., 1999. The location of infinite electrodes in pole-pole electrical surveys: consequences for 2D imaging. Journal of Applied Geophysics, 41: 313-333.

Sasaki, Y., 1992. Resolution of resistivity tomography inferred from numerical simulation. Geophysical Prospecting, 40: 453-464.

Seaton, W.J., and Burbey, T.J., 2000, Aquifer characterization in the Blue Ridge physiographic province using resistivity profiling and borehole geophysics: geologic analysis. Jour. of Environmental and Engineering Geophysics, v. 5., issue 3, p. 45-58.

Stewart, J.W., 1962, Water-yielding potential of weathered crystalline rocks at the Georgia Nuclear Laboratory: U.S. Geological Survey Professional paper 450-B, p.106-107

Stewart, J.W., Callahan, J.T., Carter, R.F., 1964, Geologic and hydrologic investigation at the site of the Georgia Nuclear Laboratory, Dawson County, Georgia: U.S. Geological Survey Bulletin 1133-F

Walsh-Stovall, C.A., Dove, P.M., and Bartholomew, M.J., 2000, Geologic map of the Check quadrangle: Virginia Division of Mineral Resources, unpublished digital manuscript map

APPENDIX A

Resistivity data collection parameters

All profiles were collected using the dipole-dipole method. The "a" spacing is expressed as multiples of the electrode spacing. Values for "n" are multiples of the "a" spacing.

Profiles with 25 electrodes

"a" spacing	"n" value
1	1-6
2	3-6
3	4-6

Total of 178 resistivity measurements

Profiles with 50 electrodes

"a" spacing	"n" value
1	1-6
2	3-6
3	4-6
4	5-6
5	5-6
6	5-6

Total of 578 resistivity measurements

APPENDIX B

All profiles were collected with a 25-electrode cable.
ES=electrode spacing

Wenner Profiles

All possible measurements were taken.

"a" spacing	number of measurements
1ES	22
2ES	19
3ES	16
4ES	13
5ES	10
6ES	7
7ES	4
8ES	1

Total of 92 measurements

Schlumberger Profiles

"a" spacing	"n" value	number of measurements
1ES	1	22
1ES	2	20
1ES	3	18
1ES	4	16
1ES	5	14
1ES	6	12
2ES	3	11
2ES	4	7
2ES	5	3
3ES	3	4

Total of 128 measurements

Dipole-dipole Profiles

"a" spacing	"n" value	number of measurements
1ES	1	22
1ES	2	21
1ES	3	20
1ES	4	19
1ES	5	18
1ES	6	17
2ES	3	15

2ES	4	13
2ES	5	11
2ES	6	9
3ES	4	7
3ES	5	4
3ES	6	1

Total of 177 measurements

<u>Pole-pole Profile (2 meter electrode spacing only)</u>

"a" spacing	number of measurements
1ES	24
2ES	23
3ES	22
4ES	21
5ES	20
6ES	19
7ES	18
8ES	17
9ES	16
10ES	15
11ES	14
12ES	13
13ES	12
14ES	11

Total of 244 measurements

APPENDIX C

Inversion settings

Initial damping factor - 0.1600
Minimum damping factor - 0.0100
Line search option - 2
Convergence limit - 5.0000
Minimum change in RMS error - 0.4000
Number of iterations - 6
Vertical to horizontal flatness filter ratio - 1.0
Model for increase in thickness of layers - 10
Number of nodes between adjacent electrodes - 2
Flatness filter type - none
Reduce number of topographical datum points? - no
Carry out topography modeling? - yes
Type of topography trend removal - 1
Type of Jacobian matrix calculation - 2
Increase of damping factor with depth - 1.20
Type of topographical modeling - 0
Robust data constrain? - yes
Cutoff factor for data constrain - 0.050
Robust model constrain? - yes
Cutoff factor for model constrain - 0.0020
Allow number of model parameters to exceed datum points? - yes
Use extended model? - no
Reduce effect of side blocks? - no
Type of mesh - 0
Optimize damping factor? - no
Time-lapse inversion constrain - 2
Type of time-lapse inversion method - 0
Thickness of first layer - 0.50
Factor to increase thickness layer with depth - 1.10

APPENDIX D

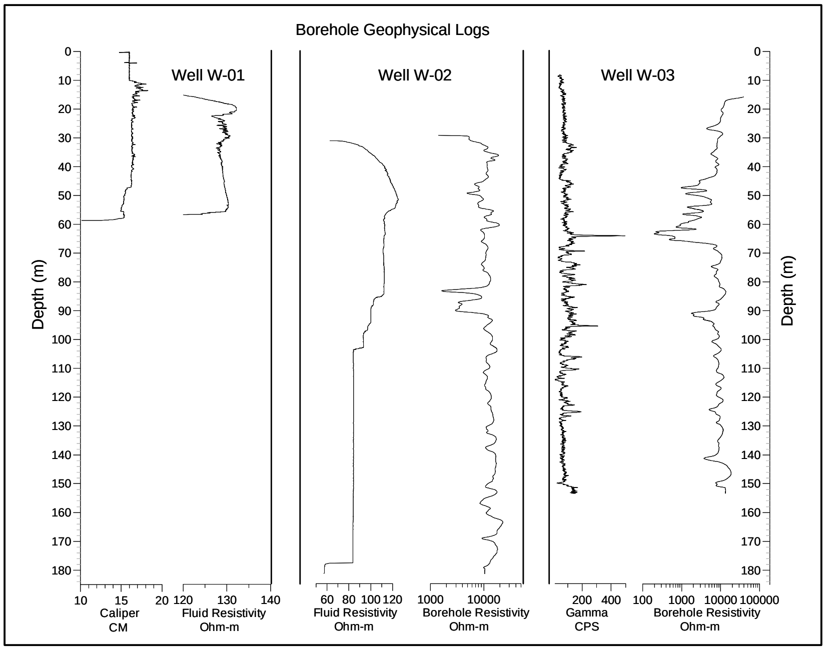
Borehole Geophysical Logs
Well W-01
Well W-02
Well W-03
Depth (m)
Caliper
CM
Fluid Resistivity
Ohm-m
Borehole Resistivity
Ohm-m
Gamma
CPS

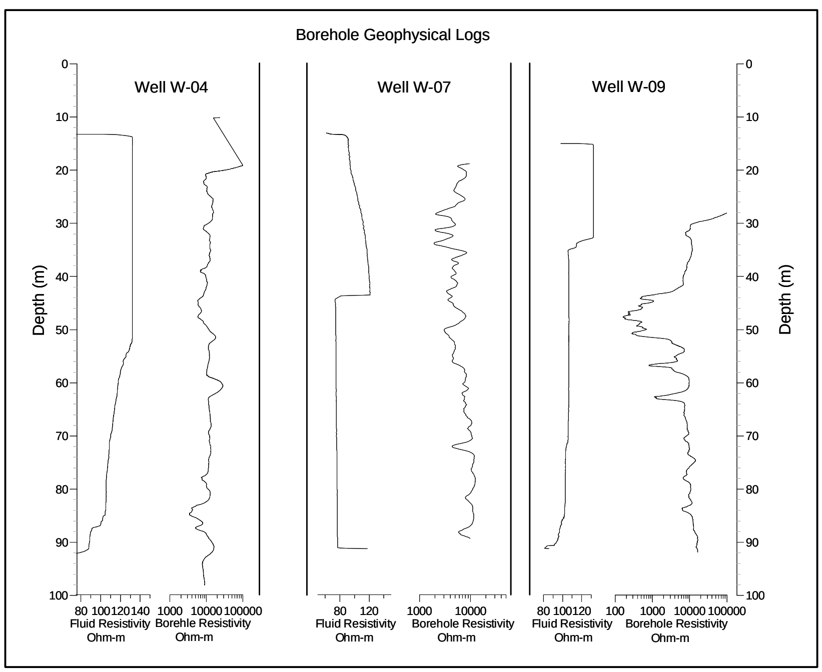
Borehole Geophysical Logs
Well W-04
Well W-07
Well W-09
Depth (m)
Fluid Resistivity
Ohm-m
Borehle Resistivity
Ohm-m
Borehole Resistivity
Ohm-m

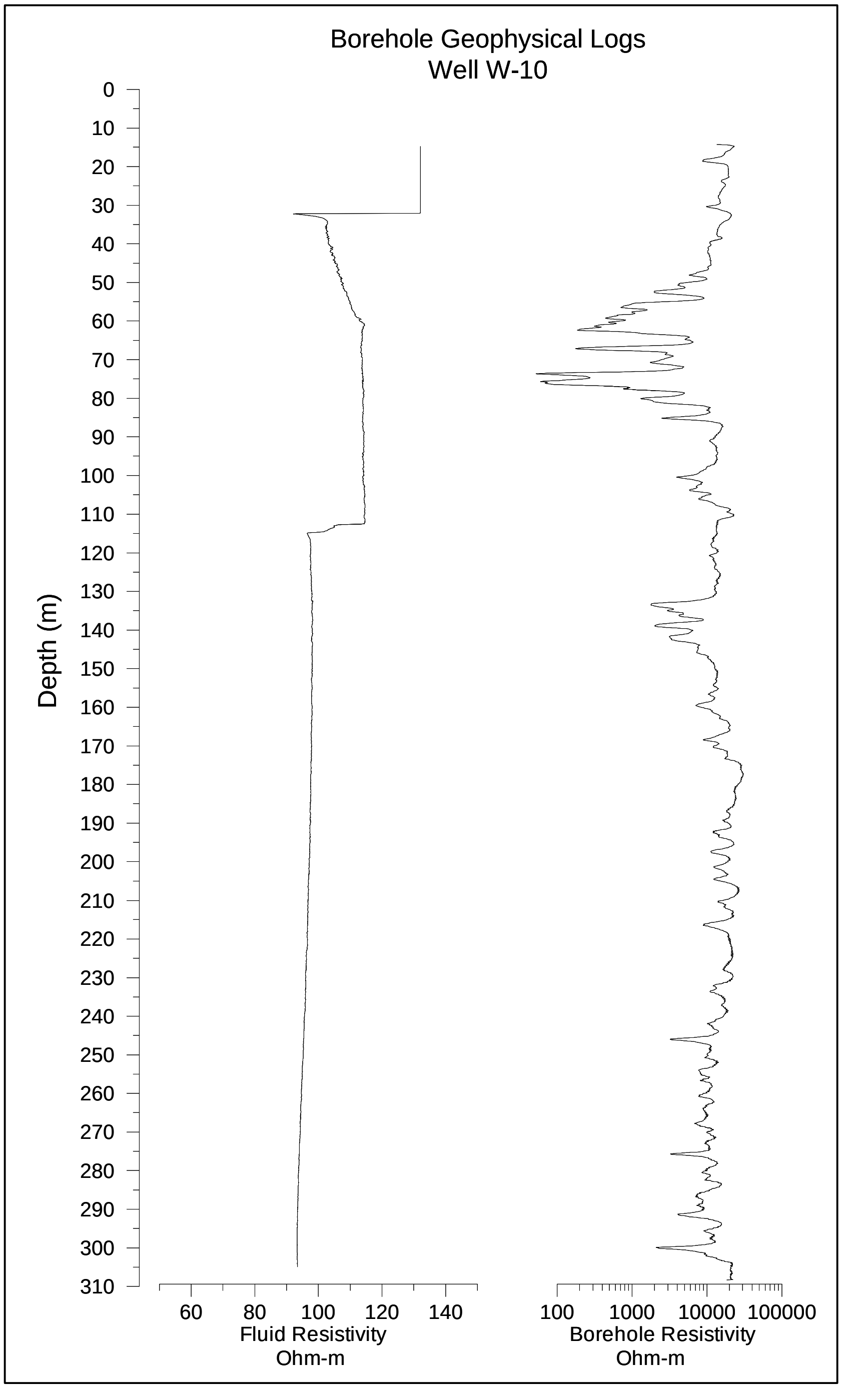

Borehole Geophysical Logs
Well W-10
Depth (m)
0
10
20
30
40
50
60
70
80
90
100
110
120
130
140
150
160
170
180
190
200
210
220
230
240
250
260
270
280
290
300
310
60
80
100
120
140
Fluid Resistivity
Ohm-m
100
1000
10000
100000
Borehole Resistivity
Ohm-m

VITA

Name: William J. Seaton
Born: June 25, 1955, Syracuse, New York

Academic and Professional Positions

1998-present: Consulting Geologist, Advanced Technical Services International, Inc., Christiansburg, VA
1994-1997 (during school breaks): Hydrogeologist, Environmental Systems and Technologies, Blacksburg, VA.
1994-present: Ph.D. Candidate, Geological Sciences, Virginia Tech, Blacksburg, VA.
1980-1994: Geologist, Phillips Petroleum Company, Houston, TX.
1979: Geologist, Lone Star Cement Company, Daleville, Virginia

Education:

B.A. Liberal Arts (Geology, Physics majors), State University College, Potsdam, NY, May 1977
M.S. Geological Sciences, Virginia Tech, Blacksburg, Virginia, May 1982

Selected Publications

Seaton, W.J. and Burbey, T.J. 2002, Evaluation of two-dimensional resistivity methods in a fractured crystalline rock terrane, Journal of Applied Geophysics, in review.

Seaton, W.J. and Burbey, T.J. 2000, Aquifer Characterization in the Blue Ridge Physiographic Province Using Resistivity Profiling and Borehole Geophysics: Geologic Analysis, Journal of Environmental and Engineering Geophysics, vol. 5, no. 3, p 45-58.

Burbey, T.J. and Seaton, W.J., 1999, Evidence for a New Hydrogeologic Model for the Blue Ridge and Piedmont Provinces, 1999 Virginia Water Research Symposium Proceedings, J.A. Poff and L. Shabman editors, Virginia Water Resources Research Center, Blacksburg, Va., 156 p.

Seaton, W.J., 1999, Aquifer Protection in the Fractured Crystalline Rocks of the Blue Ridge Province, Floyd County, Virginia, (abstract) 12th Annual Virginia Water Conference, Virginia Lakes and Watersheds Association, Fredericksburg, VA.

Seaton, W.J., 1997, Shallow subsurface geophysical study along the Mountain Run Fault in Albemarle County, Virginia, (abstract) Virginia Academy of Science 75th Annual Meeting, Blacksburg, VA.

Dean, W.T., Johnson, J.A., Seaton, W.J., Fagan, B.J., Fenstermacher, J.M., 1997, Use of computer modeling to aid in hydraulic barrier design, Conference Proceedings, International Containment Technology Conference, St. Petersburg, Fla.

Seaton, W.J., 1996, Effects of bedrock geology on water well yields and water chemistry in the Blue Ridge and Piedmont Provinces of Virginia (abstract) 9th Annual Virginia Water Conference, Virginia Lakes and Watersheds Association, Staunton, VA.

Johnson, J.A. and M.A. Parcher, J.C. Parker, and W.J. Seaton, 1996, VOC Vapor Transport: Implications for Risk Assessment, Proc. Conference on Petroleum Hydrocarbons and Organic Chemicals in Ground Water: Prevention, Detection, and Remediation, Houston, TX, API/NGWA

Seaton, W.J., 1991, Direct Detection of Porosity in the Smackover Formation at Chatom Field, Washington County, Alabama (abstract) 7th Annual Gulf Coast Exploration & Development Meeting & Exposition of the SEG, New Orleans, LA.